Progress in Oceanography 138 (2015) 504–520

Contents lists available at ScienceDirect

Progress in Oceanography

journal homepage: www.elsevier.com/locate/pocean

An individual-based model of the krill *Euphausia pacifica* in the California Current

Jeffrey G. Dorman [a,b,*], William J. Sydeman [b], Steven J. Bograd [c], Thomas M. Powell [a]

[a] University of California, Berkeley, United States
[b] Farallon Institute for Advanced Ecosystem Research, United States
[c] NOAA, Southwest Fisheries Science Center, United States

ARTICLE INFO

Article history:
Available online 2 April 2015

ABSTRACT

Euphausia pacifica is an abundant and important prey resource for numerous predators of the California Current and elsewhere in the North Pacific. We developed an individual-based model (IBM) for *E. pacifica* to study its bioenergetics (growth, stage development, reproduction, and mortality) under constant/ideal conditions as well as under varying ocean conditions and food resources. To model *E. pacifica* under varying conditions, we coupled the IBM to an oceanographic-ecosystem model over the period 2000–2008 (9 years). Model results under constant/ideal food conditions compare favorably with experimental studies conducted under food unlimited conditions. Under more realistic variable oceanographic conditions, mean growth rates over the continental shelf were positive only when individuals migrated diurnally to the depth of maximum phytoplankton layer during nighttime feeding. Our model only used phytoplankton as prey and coastal growth rates were lower than expected (0.01 mm d^{-1}), suggesting that a diverse prey base (zooplankton, protists, marine snow) may be required to facilitate growth and survival of modeled *E. pacifica* in the coastal environment. This coupled IBM–ROMS modeling framework and its parameters provides a tool for understanding the biology and ecology of *E. pacifica* and could be developed to further the understanding of climatic effects on this key prey species and enhance an ecosystem approach to fisheries and wildlife management in this region.

Introduction

Krill are considered to be a key trophic link in the transfer of energy from primary production to commercially and recreationally important predators such as hake, salmon, and seabirds in the California Current Ecosystem (CCE; Field et al., 2006). The krill species *Euphausia pacifica* is the most abundant euphausiid in the CCE and represents substantial primary consumer biomass in the region (Brinton, 1962). *E. pacifica* are abundant year-round in the central-northern CCE, although the majority of growth and reproduction is thought to occur in the spring and summer in association with upwelling (Smiles and Pearcy, 1971; Feinberg and Peterson, 2003; Shaw et al., 2010). Recent years of low krill abundances (including *E. pacifica*) contributed to the collapse of certain predators of the region (Cassin's auklet, Chinook salmon) (Sydeman et al., 2006; Lindley et al., 2009) and highlight the need to model krill populations and consider predator–prey interactions in fisheries and marine wildlife management (Field and Francis, 2006; Batchelder and Powell, 2002).

Fortunately, there has been much research on the population biology of *Euphausia pacifica*. The timing and variability of stage development under maximum food conditions and at various temperatures have been studied experimentally by Ross (1981) and Feinberg et al. (2006). Direct measurements of growth, molt, reproduction, and metabolism over a range of stages and weights are available for modeling energy budgets (Ross, 1982a,b). Experimental work on ingestion rates and food preferences also provide information on energetics under food-limited conditions (Ohman, 1984). Information on reproductive parameters (brood size, inter-brood period, egg hatching success) is available from both field (Feinberg and Peterson, 2003; Gómez-Gutiérrez et al., 2006, 2007) and laboratory work (Ross et al., 1982; Feinberg et al., 2007). Field studies using depth-specific net sampling has clarified vertical migration patterns of adults, the lack of vertical migration in young larval stages, and the variability that exists in older larval stages (Bollens et al., 1992). Field-work has also provided a reasonable understanding of the population size structure and growth rates of individual cohorts (Brinton, 1976; Smiles and Pearcy, 1971; Bollens et al., 1992; Shaw et al., 2009). This research provides a strong foundation to parameterize a bioenergetic individual-based model (IBM) for *E. pacifica* in the CCE.

* Corresponding author at: Farallon Institute for Advanced Ecosystem Research, United States.
E-mail address: jdorman@faralloninstitute.org (J.G. Dorman).

http://dx.doi.org/10.1016/j.pocean.2015.02.006
0079-6611/

Synthesis of the literature on *Euphausia pacifica* reveals an organism with a highly variable life history. This variability can be incorporated into individual-based models through parameter or life-stage variability. This is important for the CCE, an ecosystem characterized by strong temporal environmental variability (Checkley and Barth, 2009). While traditional compartmentalized ecosystem models have increased in complexity to include multiple components of nutrients, phytoplankton, and zooplankton (e.g., NEMURO: Kishi et al., 2007 and CoSiNE: (Chai et al., 2002, 2009), these models are limited in their ability to integrate individual-scale variability and behavior, such as diurnal vertical migration. Notably, IBMs provide greater resolution to population-level processes, yet provide less information on entire zooplankton communities. Nonetheless, if the species being modeled is of critical importance within an ecosystem (e.g., key to predator–prey interactions, as is the case here), modeling a single species may provide great insight into broad-scale ecosystem dynamics.

Here, we describe and analyze an IBM developed for *Euphausia pacifica*, with emphasis on comparing model results to experimental and field observed life history parameters. We hypothesize that the IBM will produce realistic population biology characteristics for *E. pacifica*. To test this hypothesis we compared model results under ideal (food unlimited) conditions to experimental results. We also compared model results under realistic ocean conditions to field observations. To obtain realistic ocean conditions, we couple the IBM with a 3-dimensional ocean circulation model (Regional Ocean Modeling System, ROMS) and ecosystem model (Nutrient, Phytoplankton, Zooplankton, Detritus; NPZD). As no one-year in the CCE is the same, to obtain a robust climatology of realistic ocean conditions in this highly variable ecosystem, we modeled the system over 9 years. These results lay the groundwork for future modeling efforts of *E. pacifica* in the CCE and elsewhere in the North Pacific where this species occurs and is critical to ecosystem functions.

Methods

Our IBM of *Euphausia pacifica* is built upon the POPCYCLE model (Batchelder and Miller, 1989; Batchelder et al., 2002). *E. pacifica* bioenergetics are dependent on sex, size, life stage, and environmental conditions (temperature and food concentrations), which are imported from the coupled physical oceanographic and ecosystem model.

Growth of non-feeding stages

The egg stage and first two life stages (naupliar I and II) of *Euphausia pacifica* are non-feeding and influenced by temperature alone. Temperature-dependent development is implemented using physiological-time, calculated as the temperature an individual is exposed to (°C) multiplied by the time-step duration (days). The sum of an individual's physiological-time is thus a measure of the temperature history for each individual.

Egg hatching time for *Euphausia pacifica* is implemented based on experimental work showing 50% of eggs hatching by day 1.625 at 10.5 °C (physiological-time = 17.1 degree days) (Feinberg et al., 2006). Naupliar stage growth depends on yolk reserves. Physiological-time from hatch to metanauplius stage is calculated by averaging 8 °C and 12 °C stage development data from Ross (1981). Total physiological-time to the first feeding stage is 38.3 degree days. During this period, respiration of eggs and naupliar stages is implemented based on stage dependent mass (Ross, 1979, Appendix II). It is expected that higher temperatures would lead to greater metabolic costs and greater weight loss rates (Gillooly et al., 2001), but experimental data of weight loss from egg to metanaupliar stage development measured at 8 °C (0.21 μg C d^{-1}) and 12 °C (0.16 μg C d^{-1}) did not support this expectation. We assume that this difference is due to measurement error (variance of data not reported) and our limited access to the raw data that went into the reported values in the literature. An average daily weight loss rate of 0.18 μg C d^{-1} was applied to all individuals. Development from egg to metanauplius is rapid, even at colder temperatures (less than 5 days at 8 °C), and we do not expect that this will have a significant impact our organisms over the course of an 8–12 month lifespan. Development and respiration of non-feeding stages was capped at a lower limit of 6 °C and upper limit of 16 °C.

Growth of feeding stages

Growth of all stages beyond the naupliar stages is dependent upon temperature and food resources; these variables are supplied by ROMS and NPZD output.

Maximum growth

Individual growth is modeled using the equation for growth measured directly by Ross (1982a). As Ross's growth equation was derived under food unlimited conditions, these results represent maximum growth where G_{max} = maximum growth rate (μg C d^{-1}) and W = organism weight (μg C). Eq. (1) represents maximum growth for individuals less than 12.5 μg C and Eq. (2) represents maximum growth for those greater than 12.5 μg C.

$$G_{max} = -0.315(0.198\ W) \tag{1}$$

$$G_{max} = 0.216\ W^{0.617} \tag{2}$$

Scaling maximum growth by food resources and temperature

To implement food-dependent growth, weight gain was scaled based on a relationship between the ingestion rate, critical concentration, and the food threshold at which no growth occurs. Ingestion rate is calculated using an experimentally derived equation (Eq. (3)) measured under varying food concentrations (Ohman, 1984), where I = ingestion rate, a = 1.173, T_h = handling time (0.141 s $cell^{-1}$) and X = prey concentration.

$$I = \frac{aX^2}{1 + (aT_hX^2)} \tag{3}$$

The critical concentration (CC) is the phytoplankton concentration at which an organism is able to achieve maximal growth. CC is defined as 90% of the maximum ingestion rate, and is dependent upon both organism size and temperature in our modeling study. Ross (1982a) determined CC of three size groups of *Euphausia pacifica* (<750 μg C, 750–1650 μg C, and >1650 μg C) and at two temperatures (8 °C and 12 °C). Model CC at 12 °C is calculated using Eq. (4) for individuals greater than 500 μg C and less than 2000 μg C. CC is a constant for individuals less than 500 μg C (CC = 125 μg C l^{-1}) and individuals greater than 2000 μg C (CC = 375 μg C l^{-1}).

$$CC = 41.67 + \left(\frac{W}{6}\right) \tag{4}$$

Temperature scaling of the critical concentration is determined using the mean Q_{10} value of the three size classes published by Ross (1982a, mean Q_{10} = 1.59). The results generally agree with the only other published value of a critical concentration for adult *Euphausia pacifica* (290 μg Cl^{-1}; Ohman, 1984).

A food scale factor (FSF) is determined using Eq. (5) by comparing the ingestion rate to the ingestion rate at critical concentration (I_{cc}).

$$\mathrm{FSF} = \frac{I}{I_{cc}} \tag{5}$$

Adjustment to the food scale factor is made to limit the maximum value to not exceed 1, so that growth does not exceed G_{max}. Food scale factor is also minimally limited to half of the no-growth threshold (Eqs. (6) and (7)), due to the Type III shape of the ingestion curve (Ohman, 1984), indicating a decreased feeding effort under food limiting conditions, reducing metabolic requirements.

To determine the threshold at which no growth occurs (G_{zero}), the ratio of metabolism to ingestion (i.e., % of ingestion energy accounted for via metabolism) was determined using equations from Ross (1982a). This ratio scales with weight as described by Eq. (5) for individuals less than 165 μg C and Eq. (6) for those greater than 165 μg C.

$$G_{zero} = 0.548 + (-0.0723\ W) \tag{6}$$

$$G_{zero} = 0.407 + (-0.0528\ W) \tag{7}$$

The food scale factor and no growth threshold are then applied to Eq. (8) to determine the growth (G) of the individual.

$$G = \frac{G_{max}}{1 - G_{zero}}(\mathrm{FSF} - G_{zero}) \tag{8}$$

To scale the growth increment by temperature a Q_{10} value of 3.62 was used (Ross, 1982a).

Stage development

To model life stage structure and development, 13 life stages are included in the IBM. Life stages that exhibit similar behavior have been combined together (both naupliar stages, furcilia IV and furcilia V stages, and juvenile and adult stages). Progression from one life stage to the next is dependent upon physiological time of development for egg and nauplius stages, and weight increase for all other stages. Weight gain beyond a life stage threshold (Table 1) determines progression from one stage to the next. Threshold weights were determined using midpoints between average weights of stages reported by Ross (1979, Table 19 therein). An individual that loses weight below a threshold weight does not regress back to the previous stage.

Reproduction

Reproduction is implemented based on weight-dependent reproductive effort (Ross, 1982a) (Eq. (9)). The equation for reproductive weight (R_{wt}) was derived at a full food ration and scaling of the equation with food resources is done in the same way growth is scaled. Temperature scaling is done using a Q_{10} value of 3.60, which was derived from the experimental data of Ross (1982a).

Table 1
Thresholds that individuals must progress beyond to advance to the next life-stage.

Developmental stage	Threshold	Units
Egg hatch	17.06	degree-days
Metanauplius	38.28	degree-days
Calyptopis I	2.33	μg C
Calyptopis II	3.52	μg C
Calyptopis III	6.52	μg C
Furcilia I	11.76	μg C
Furcilia II	17.70	μg C
Furcilia III	32.44	μg C
Furcilia IV–V	55.77	μg C
Furcilia VI	70.56	μg C
Furcilia VII	78.02	μg C
Juvenile–adult	84.90	μg C

$$R_{wt} = 20.37 + \left(10.29\ W\ 10^{-3}\right) \tag{9}$$

While Ross defined her equation for all organisms with a weight greater than 685 μg C, reproductive weight gain in our IBM is not implemented until organisms are 1500 μg C and is maximized when organisms reach 6000 μg C. These values roughly equate to reproduction beginning at an individual length of 13 mm and achieving a maximum reproductive effort at 21 mm length, and agree with field observations from northern California and Oregon (Dorman et al., 2005; Gómez-Gutiérrez et al., 2006). If positive growth is not achieved during the feeding process, but there is reproductive weight associated with the individual, reproductive weight is absorbed back into the body to minimize weight loss.

The release of eggs is only allowed during nighttime, between 0100 and 0300, to ensure that individuals are in surface waters where egg release is most common. Release of eggs is a function of two factors: inter-brood period (IBP) and the ratio of reproductive weight to body weight (RW:BW). IBP is the amount of time between releases of eggs and is set to 10 days. Individuals are set to release eggs every 10 days if reproductive weight is between 2.5% and 7.5% of body weight. If reproductive weight is less than 2.5% body weight and IBP is greater than 10 days, eggs are not released. If the RW:BW ratio is greater than 7.5% and the IBP is less than 10 days, eggs are released, resulting in a shorter IBP. The number of eggs released is equal to the reproductive weight divided by the average weight of an egg (2.58 μg C).

Mortality

Starvation mortality is implemented based on weight loss below 70% of each individual's maximum attained weight (see Section 'Modeling under variable ocean conditions' for discussion of parameter choice in relation to results). Predation and natural mortality rates are not well known for *Euphausia pacifica*, or any other zooplankton, and are often used as a closure term in models (Edwards and Yool, 2000). We have not implemented predation and natural mortality terms as we are not trying to model actual numbers of *E. pacifica*, and are more concerned with relative seasonal changes in the population biology.

Particle tracking

Individuals are tracked in the model using a common 4th-order Runge–Kutta method (Butcher, 2003) using u, v, and w velocities from the ROMS model. Vertical diffusivity is incorporated into vertical displacement though a non-naïve random walk (Visser, 1997) to avoid the accumulation of individuals in regions of low vertical diffusivity. Horizontal diffusivity is not implemented in particle tracking, as its impact on horizontal position is very small compared to horizontal current velocities.

Additional vertical movement is added behaviorally through diel vertical migration (DVM) of individuals. DVM is implemented in the model using light levels to determine the preferred depth of the organism in a similar fashion to Batchelder et al. (2002). Swim speed (SS) is determined by Eq. (10) with scale factors (range from 0 to 1) based on organism size (SZ), life stage dependent probability of migration (POM), distance from preferred light level (LT), and distance from surface (SB) or bottom boundary (BB), all modifying maximum swim speed (MXSS, from Torres and Childress, 1983) (Fig. 1).

$$\mathrm{SS} = \mathrm{MXSS}(\mathrm{SZ}\ \mathrm{POM}\ \mathrm{LT}\ \mathrm{SB}\ \mathrm{BB}) \tag{10}$$

Migration is only possible for organisms that are greater than life stage furcilia III as POM = 0 for younger individuals. All juvenile and adult individuals will engage in DVM (POM = 1) if other conditions are favorable. Distance from preferred light level must be

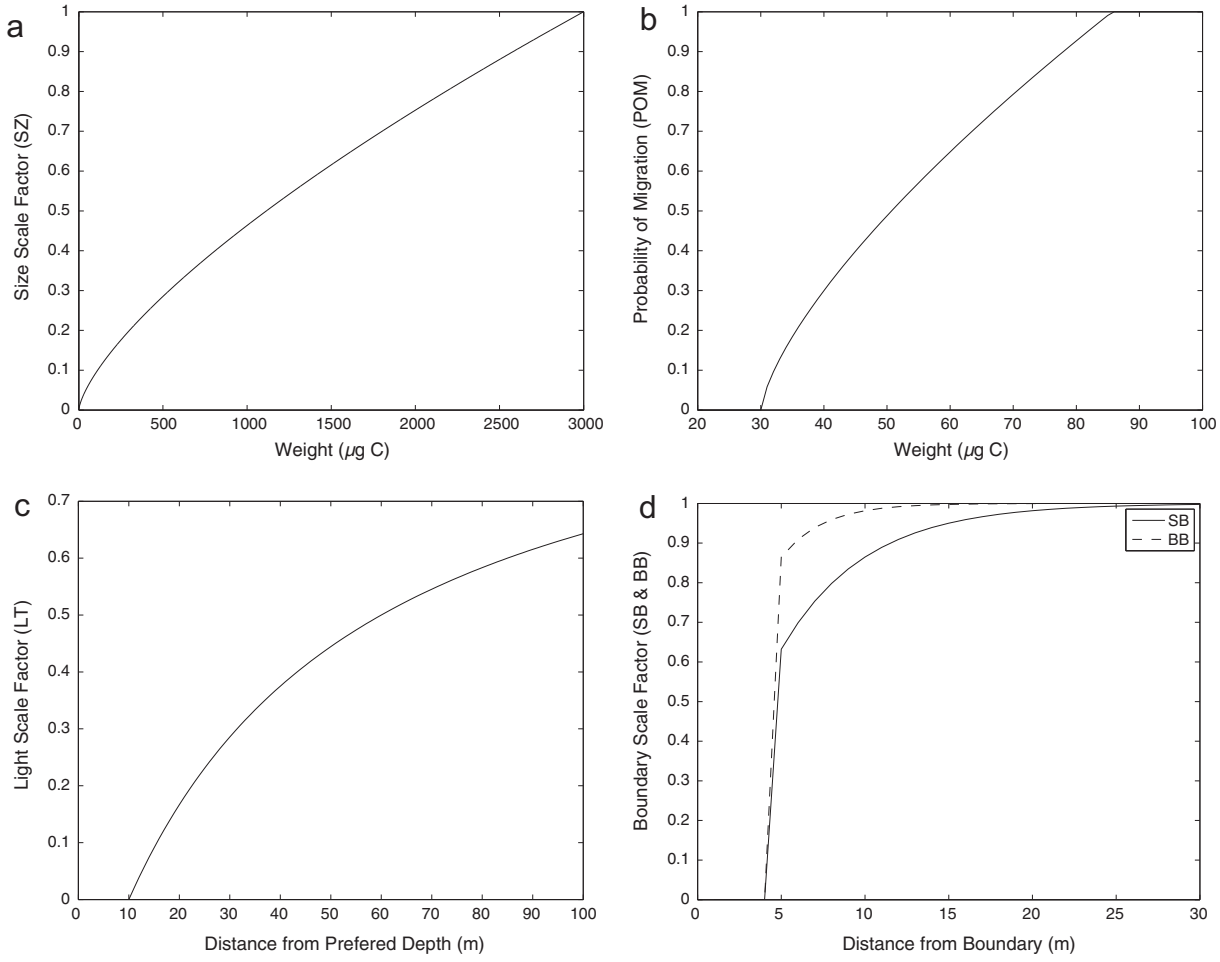

Fig. 1. Scaling factors that impact vertical migratory swimming speed based on (a) organism size, (b) life-stage (using weight as a proxy), (c) distance from preferred depth, and (d) proximity to surface and bottom boundaries.

greater than 10 m to trigger vertical migration. If the preferred light level is above the surface of the water, the preferred depth is set to 5 m. Resultant migration of adult *Euphausia pacifica*, when not constrained by bathymetry, is to approximately 160 m. Time to ascend/descend for adults is from 45 to 90 min.

Individuals that leave the model through an open boundary are labeled as such and are removed from the list of individuals that is evaluated for each time-step.

Oceanographic model interface

The IBM can be run in 3-dimensional space with physical oceanographic data from ROMS (Shchepetkin and McWilliams, 2005; Haidvogel et al., 2008). POPCYCLE interfaces with ROMS offline (i.e., model runs are not concurrent) by reading in temporal daily "snapshots" of averaged data (temperature, phytoplankton, currents, and vertical diffusivity). For each individual, the ocean data corresponding to that individual's location is spatially trilinearly interpolated to that location and temporally linearly interpolated between adjacent days.

Model simulations

Regional Ocean Modeling System (ROMS)

ROMS is commonly used to model the coastal ocean and upwelling ecosystems such as the California Current (Powell et al., 2006; Di Lorenzo et al., 2008). To model the northern California coastal region, we created a model domain from Newport, Oregon to Point Conception, California that extends approximately 1000 km offshore with grid resolution of approximately 3 km in the cross-shelf direction and 6 km in the alongshore direction (Fig. 2). An NPZD ecosystem model (Powell et al., 2006) was run concurrently with ROMS and model output was saved at daily intervals.

Forcing of ROMS is parameterized using the bulk fluxes formulation developed by Fairall et al. (1996). Atmospheric forcing data (shortwave radiation, downward-longwave radiation, air temperature, relative humidity, precipitation, and wind speed) are from the National Centers for Environmental Predictions (NCEP) North American Regional Reanalysis (NARR) database at 3-h intervals (http://www.esrl.noaa.gov/psd/data/narr/).

Physical boundary and initial conditions for the model are from the Simple Ocean Data Assimilation (SODA) model (Carton and Giese, 2008) obtained through the Asia–Pacific Data Research Center (http://apdrc.soest.hawaii.edu/). These data are interpolated from the SODA grid onto our ROMS grid using a triangle-based linear interpolation scheme based on Delaunay triangulation of the data. In certain parts of the deep ocean, differences in the grid resolution of the two models (SODA and ROMS) resulted in use of nearest-neighbor interpolation. The temporal resolution of the physical boundary conditions is monthly. Biological boundary conditions for the NPZD model are from the World Ocean Atlas and Database 2009 (National Oceanographic Data Center). Nitrate values are from a 1° resolution, monthly climatology from the World Ocean Atlas 2009. Phytoplankton density monthly

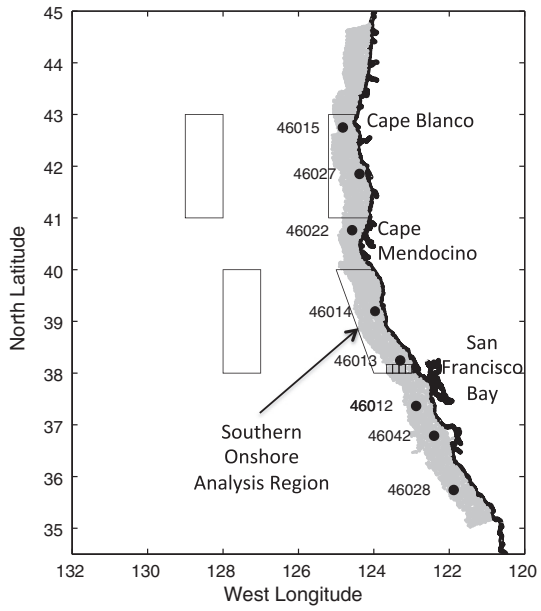

Fig. 2. Map of the study area. Black markers (•) mark locations of National Data Buoy Center Stations utilized for model data comparison. Four large boxes (northerly/southerly and onshore/offshore) are regions used for analysis of satellite data. Large southern onshore box was used for analysis of individual-based model data. Four small boxes (onshore at latitude 38) were used for analysis of CODAR data. Light-gray onshore region is the initial location of particles in the IBM.

climatology values are from World Ocean Database 2009 data that was collected within our ROMS grid from 1990 to 2009. Zooplankton and detritus density initial and boundary values were set to 10% of phytoplankton values.

The ROMS model was run for the years 2000–2008 (n = 9 years). For each year modeled, ROMS was spun up from initial conditions for 6 months, from 1 July to 31 December of the prior year. This spin up time was selected based on previous studies (Powell et al., 2006) that found this sufficient amount of time so initial physical and biological conditions did not influence model results (Powell et al., 2006). ROMS was restarted each year due to uncertainty in biological initial conditions (from Powell et al., 2006) and boundary conditions (derived from large spatial and temporal resolution). Starting from similar initial conditions reduced the possibility of drift in baseline values of biological parameters over the course of a long simulation.

Individual-based model – POPCYCLE

Modeling under ideal environmental conditions. Analyses of the bioenergetics of the IBM were carried out across a spectrum of organism weights (larval to adult) and temperatures. Development, growth rates, and reproductive output were all modeled using a full ration of food so that results would be comparable to experimental work, which is most commonly done under maximum food resources. The weights (500, 1000, 3000, and 6000 μg C) used in the text and figures to illustrate the impact of individual size on bioenergetics demands correspond to lengths of approximately 10 mm (juvenile), 12 mm (small adult), 17 mm (adult), and 22 mm (large adult). Temperatures in the figures explore the full range of bioenergetics response. We refer to 8 °C and 12 °C in the text as there often is accompanying experimental data at these temperatures to compare with and these values are within the natural range of temperatures experienced by *Euphausia pacifica* in our region of interest.

Modeling under variable ocean conditions. Modeling *Euphausia pacifica* using the IBM in 3-dimensional space was done using ROMS output from 2000 to 2008. Two "suites" of model runs were completed with each suite consisting of 54 runs, 6 per year over the 9 years. Each model run lasted for 60 days. Model start dates were the first day of February, April, June, August, October, and December. For each model run, ~10,500 individuals (particles) were uniformly seeded within 60 km of the coastline between a depth of 5 and 30 m (Fig. 2). All individuals were placed in the domain as adults (3000 μg carbon weight, approx. 17.5 mm length). One "suite" of runs parameterized the upper limit of DVM at 0–10 m (i.e., surface, hereafter referred to as "surface DVM"), while the other "suite" parameterized the upper limit of DVM to the local chlorophyll *a* maximum at the time of ascent (hereafter referred to as "maximum-food DVM").

Data analysis

To validate ROMS, associations between monthly averaged sea-surface temperature (SST), alongshore and cross-shelf currents, and chlorophyll *a* from modeled output and observations were conducted using Pearson correlations. The residuals were examined for autocorrelation and accounted for using a single iteration of the Cochrane–Orcutt method if necessary. For these comparisons, SST was obtained from 8 National Data Buoy Center coastal stations (http://www.ndbc.noaa.gov/) (Fig. 2). Monthly averaged alongshore and cross-shelf surface currents were collected using high-frequency radar (CODAR) obtained from the Bodega Ocean Observing Node (BOON, http://bml.ucdavis.edu/boon/partners.html). The data were averaged into 1/6th degree bins across the continental shelf just north of Pt. Reyes, CA (Fig. 2). Monthly chlorophyll *a* satellite data (Kahru et al., 2009) were binned from two coastal and two offshore domains in the northern and southern part of the ROMS model (Fig. 2).

Interannual variability in growth rate, reproduction, and population retention were analyzed using a 2-way analysis of variance (ANOVA) using year as the primary variable and month as a nuisance variable. Growth rate anomaly was calculated by removing monthly mean growth rate values from the data and a one-way ANOVA was run on the anomaly data. A Bonferroni test (Zar, 1999) was utilized to determine specific year-to-year differences in growth rate.

Data that are presented from the IBM coupled with ROMS were almost exclusively from the coastal region (over the continental shelf) between 38 and 40 N latitude. This region was selected for analysis, as it is central to the model domain and thus less likely to be influenced by initial and boundary conditions. The only figure that uses data from beyond this analysis region is Fig. 15, which presents data from the model boundaries (north/south), and at a prescribed distance form the coast. Time series figures (Figs. 9a and b, 12a and 13a and b) were created by taking an average of all data within the analysis region for each saved time-step (every 5 days) of the model. Seasonal (bi-monthly) box-plot figures (Figs. 10a and b, 12b and 14a and b) were created from statistics on data from all years (2000–2008), within the analysis region, and during the 2-month bins in the figures. Spatial plots (Figs. 11a and b and 12c) were created by averaging all data within each ROMS grid cell during the stated time period in the figure legend. Further information on the data processing for each coupled IBM–ROMS figure (Figs. 9–16) is included in the figure captions.

The suite of model runs that began on April 1 were chosen for Figs. 11 and 12c because they are close to the time of peak upwelling in the central part of our model domain (northern California region). Finally, Appendix A was used for conversion of model growth rates (μg C d^{-1}) to units compatible with field data on growth rates of *Euphausia pacifica* (mm d^{-1}).

Results

Modeling under ideal environmental conditions

Development

At 8 °C and 12 °C, development from egg to the metanauplius stage takes 4.8 and 3.2 days and initial metanauplius weight is 1.70 μg C and 1.99 μg C, respectively (Fig. 3a). No experimental data on developmental rates from egg to metanauplius stage are available for comparison with model results, but metanauplius weights are similar to experimental weights of 1.58 μg C and 2.08 μg C. Development from egg to juvenile stage took approximately 38 days at 8 °C and 60 days at 12 °C. Model development was slightly faster than experimental results (by 0.9 days at 8 °C, by 7.0 days at 10.5 °C, and by 1.1 days at 12 °C (Fig. 3b). Development from egg to a reproductive adult (12 mm) took 130 and 210 days at 8 °C and 12 °C, respectively (Fig. 3c). Development to larger adults (>17 mm) took over a full year in 8 °C water and over 200 days in 12 °C.

Growth

Minimum food resources to achieve some level of growth ranged from a minimum value of 0.73 μg chlorophyll *a* at 8 °C to 0.80 μg chlorophyll *a* at 12 °C for an organism of 500 μg C and from 1.01 μg chlorophyll *a* at 8 °C and 1.04 μg chlorophyll *a* at 12 °C for organisms greater than 3000 μg C (Fig. 4a). Critical concentration (the food resources needed for maximum growth) increases from a minimum value of 1.73 μg chlorophyll *a* at 8 °C to 2.08 μg chlorophyll *a* at 12 °C for organisms 500 μg C, and from 5.20 μg at 8 °C and 6.25 μg at 12 °C for organisms greater than 3000 μg C (Fig. 4b). Growth rates did not differ markedly among different size classes of adults and were approximately 0.04 and 0.06 mm d^{-1} at 8 °C and 12 °C (Fig. 4c).

Reproduction

Reproduction under maximum food conditions ranges from 7 eggs per day at 8 °C to 12 eggs per day at 12 °C for a small adult (Fig. 5a) and from 19 to 32 eggs per day from 8 °C to 12 °C for a large adult. Brood size averaged 34 eggs at 8 °C or 12 °C for a small adult and 194 for a large adult (Fig. 5b). The inter-brood period shortened from 5 to 3 days for small adults and from 10 to 6 days for large adults at 8 °C and 12 °C, respectively (Fig. 5c).

Mortality

Starvation of individuals under no food conditions and a body weight of 12 μg C, which is the breakpoint at which Ross' allometric equations for growth change from linear to exponential, was approximately 11 days at 8 °C and 9 days at 12 °C (Fig. 6). Starvation of older furcilia larvae (85 μg C) was approximately 50 days at 8 °C and 30 days at 12 °C. Starvation of the smallest adults did not drop below 60 days. In the model the maximum starvation time was not allowed to exceed 200 days.

Modeling under variable ocean conditions

ROMS

Correlation of ROMS-modeled and observed SST was significant ($p < 0.001$) at all stations examined (Fig. 7a and b; $r = 0.5–0.7$). Modeled and observed alongshore transport was also significant ($p < 0.001$) in all regions (Fig. 7c and d; $r = 0.6–0.7$ for inshore locations and $r = 0.3–0.5$ at offshore locations). Modeled and observed surface phytoplankton (i.e., chlorophyll *a*) were positively correlated ($p < 0.001$), (Fig. 7e and f, $r = 0.3–0.6$). Modeled phytoplankton showed greater variability and in general slightly overestimated surface chlorophyll *a* concentrations. Discrepancies that occur in the modeled and observed data are likely the result of our forcing winds (NCEP–NARR) not matching the observed winds when at their strongest intensity (Dorman, 2011). This is due to the spatial resolution of the forcing data (32 km) not being small enough to capture the full extent of the coastal intensification of upwelling

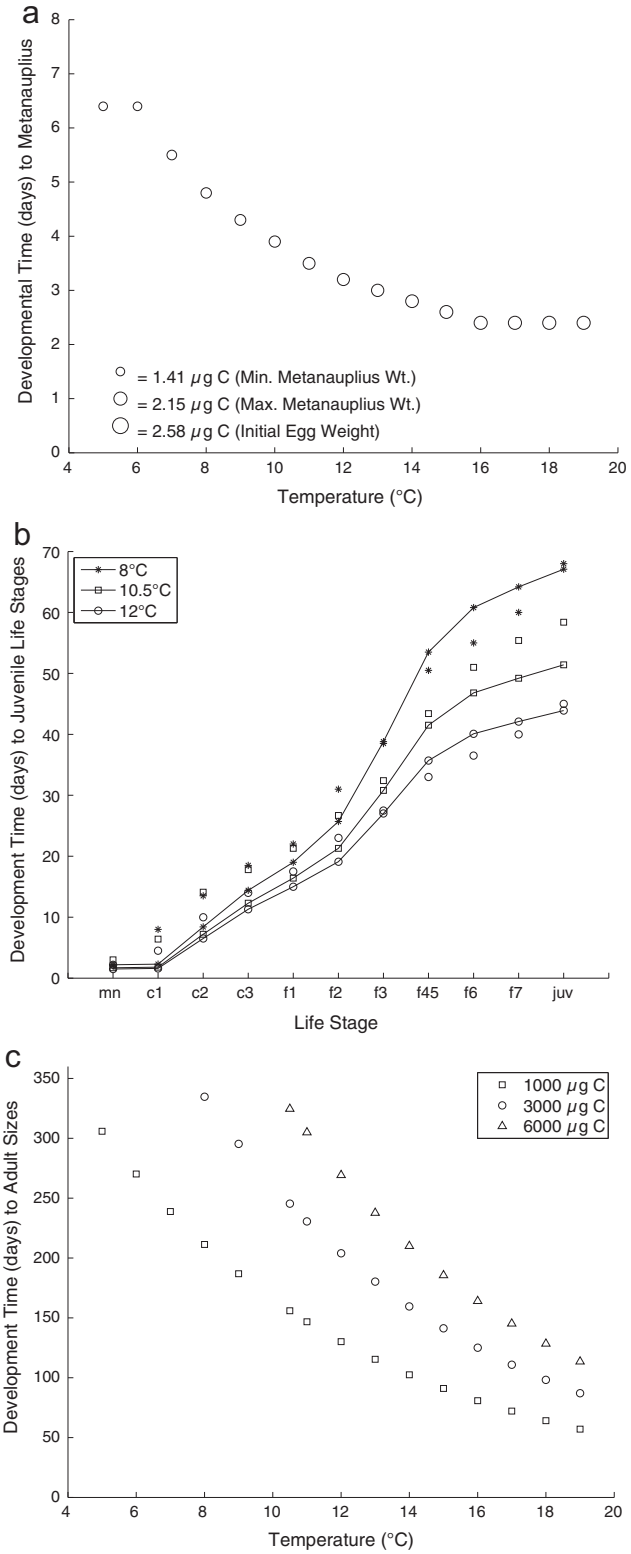

Fig. 3. Developmental time of *Euphausia pacifica* across a range of temperatures to (a) metanauplius life-stage, (b) juvenile life-stages and (c) various sizes of adult. All results are derived under maximum growth conditions (full-food ration).

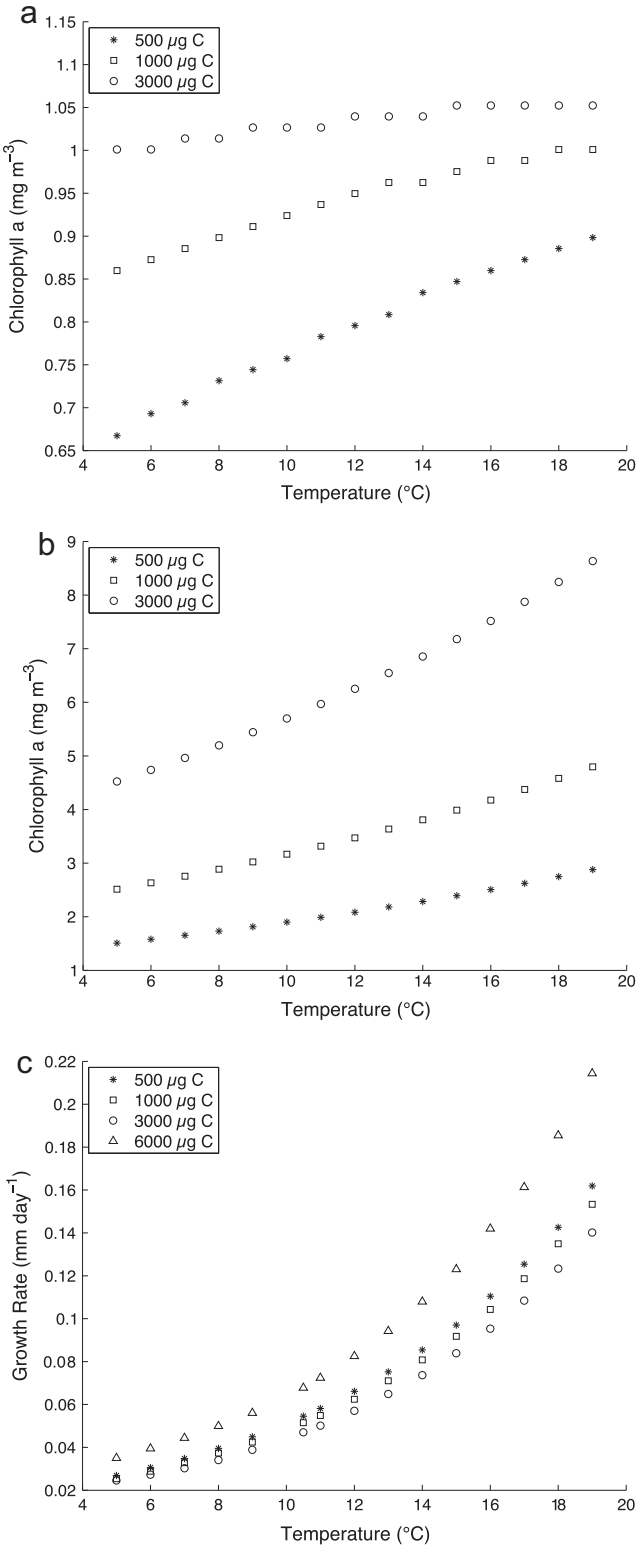

Fig. 4. Chlorophyll *a* concentration needed to (a) meet respiratory costs (growth = 0) and (b) achieve maximum growth across a range of temperatures. (c) Maximum growth rates of various sized adults across a range of temperatures.

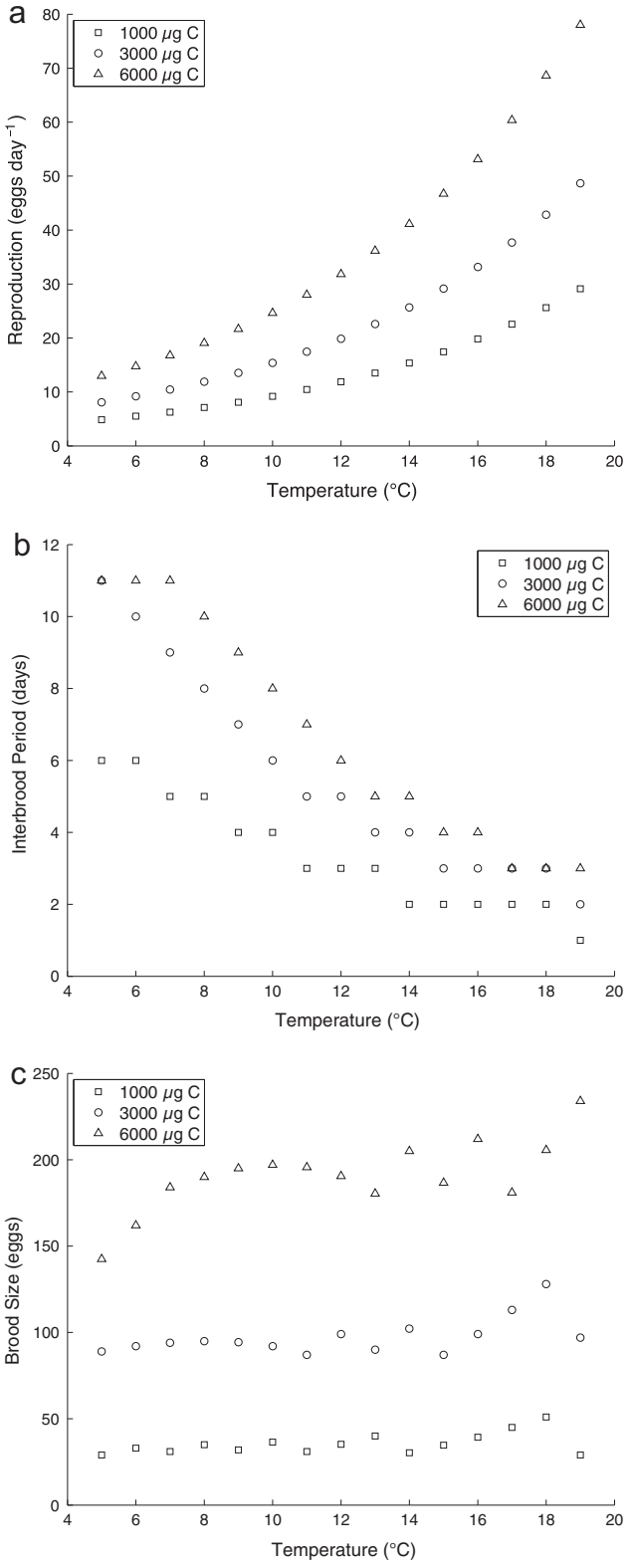

Fig. 5. Reproduction results: (a) egg production, (b) inter-brood period, and (c) brood size derived at a full-food ration across a range of temperatures.

favorable winds that is common along this coastline (Dorman and Winant, 1995).

Depth profiles of average monthly temperature and chlorophyll *a* (Fig. 8) show the seasonal cycle of upwelling in the northern California Current. Coldest surface temperatures and greatest surface chlorophyll *a* concentrations are observed in April when upwelling is strongest. Surface temperatures are warmest in July and October, increasing stratification and decreasing surface chlorophyll *a* concentration. A subsurface chlorophyll *a* maximum is observed year round, but strongest during the summer/fall months.

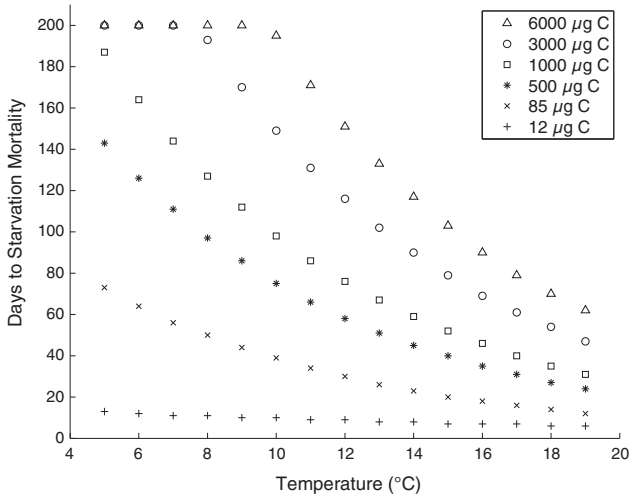

Fig. 6. Time to starvation mortality under no-food conditions across a range of temperatures for various sized individuals.

Growth

Mean growth rates of surface DVM model runs were negative throughout the modeled years (Fig. 9a) and across the seasonal cycle (Fig. 10a). While negative growth has been measured in *Euphausia pacifica* populations (Marinovic and Mangel, 1999; Shaw et al., 2010), consistent negative growth for greater than 75% of the population is unrealistic (Fig. 10a). For this reason, the majority of our analysis and discussion centers on the maximum-food DVM model runs.

Mean growth rates of maximum-food DVM model runs were generally positive year-round (Figs. 9b and 10b). Onshore growth was approximately 0.01 mm d^{-1} and offshore growth (data not shown) was close to zero. Bi-monthly or seasonal differences in mean growth rate were minimal, although there was much greater variability in growth during the fall and winter months (Figs. 9 and 10). Median growth rates of maximum-food DVM runs ranged from 0.0088 to 0.0143 mm d^{-1}. Spatially, there was higher growth over the continental shelf, including a very narrow band of high growth close to shore where growth rates averaged greater than 0.03 mm d^{-1} (Fig. 11). ANOVA results on growth rates of maximum-food DVM model runs, indicated significant differences in interannual growth rate ($F = 2.83$, $df = 8$, $p < 0.01$) and growth rate anomaly ($F = 2.87$, $df = 8$, $p < 0.01$). Using the Bonferroni method to compare growth rate anomaly between all years found that 2004 and 2007 were the only years with a significant difference in growth rate from each other ($t = 3.83$, $p < 0.05$).

Short time scale (5-day) periods of high growth were associated with lower SST and stronger southerly alongshore-surface currents (Fig. 16). Median SST during the periods of fastest euphausiid growth (largest 25th percentile of measured growth rates) was 9.6 C, compared to 11.9 C during the periods of slowest growth (smallest 25th percentile of measured growth rates). Median alongshore current during the periods of fastest euphausiid growth was −0.12 m s^{-1}, compared to −0.02 m s^{-1} during the periods of slowest growth.

Reproduction

Reproductive output was low and intermittent during the surface DVM model runs (data not shown), but was more productive and consistent during maximum-food DVM model runs (Fig. 12). Medians of bi-monthly egg production from maximum-food DVM runs ranged from 3.4 to 6.3 eggs $individual^{-1}$, with maximum periods of reproduction producing almost 20 eggs $individual^{-1}$. The number of reproductive events was much greater over the continental shelf, associated with greater food resources in the nearshore environment. Peak locations of reproduction, having more than 100 reproduction events over the course of the model runs, occurred to the north of the headlands Cape Blanco (∼latitude 42.5 N) and Cape Mendocino (∼latitude 40 N) and in the Gulf of the Farallones region, just offshore of San Francisco Bay. ANOVA results found no significant differences in reproductive output between years and increases in reproductive events were not associated with lower SST and greater southerly alongshore-surface currents (data not shown).

Mortality

Starvation mortality did not occur during these model runs as the model run time was only 60 days, shorter than the fastest time to starvation of adults under a typical temperature regime.

Advection

Particle loss from the coastal domain was greater during surface DVM runs than during maximum-food DVM runs (Fig. 13). Median particle losses of bi-monthly data were all than 15% of the population when migrating organisms to the surface and ranged from 5% to 10% loss during maximum-food DVM runs. ANOVA results found no significant interannual variability in retention and there was no significant bi-monthly/seasonal trend in particle retention from within our analysis region (Fig. 14).

Decreased particle retention (greater advection) was associated with lower SST and stronger southerly alongshore-surface currents (Fig. 16). Median SST during the periods of greatest particle loss (lower 25th percentile of measured retention values) was 10.5 C, compared to 11.2 C during the periods of greatest particle retention (upper 25th percentile of measured retention values). Median alongshore current during the periods of greatest particle loss was −0.10 m s^{-1}, compared to −0.06 m s^{-1} during the periods of greatest retention. Advection of particles out of the northern boundary was greatest for runs beginning in December and virtually non-existent for model runs beginning during April, June, and August (Fig. 15a). There was consistent advection of particles from the domain to the south and west (Fig. 15b and c) during these months.

Discussion

Modeling under ideal environmental conditions

Development

Stage development in the model progressed in a similar fashion to published results (Ross, 1981; Feinberg et al., 2006). Development through calyptopis and early furcilia stages progresses more rapidly in the model than in laboratory studies, yet with variability within bounds found in the field (Ross, 1979; Feinberg et al., 2006); the timing of modeled stage progression also is within measured variability. These developmental differences, while minor, might impact studies that rely heavily on stage-specific parameter values (e.g., mortality), but the majority of the parameters used in our study are weight-based so this is not of concern.

Growth

A comparison of model results under maximum food resources to field measurements indicates model output within the range of field observations. Average adult growth rates of 0.02 and 0.03 mm d^{-1} (with a range from −0.07 to 0.14 mm d^{-1}) have been reported for two regions off of Oregon during the summer upwelling season with food sources ranging from approximately 2 to 8 μg chlorophyll a l^{-1} (Shaw et al., 2009). A year-round study from the same region found average annual growth rates of 0.01 mm d^{-1}

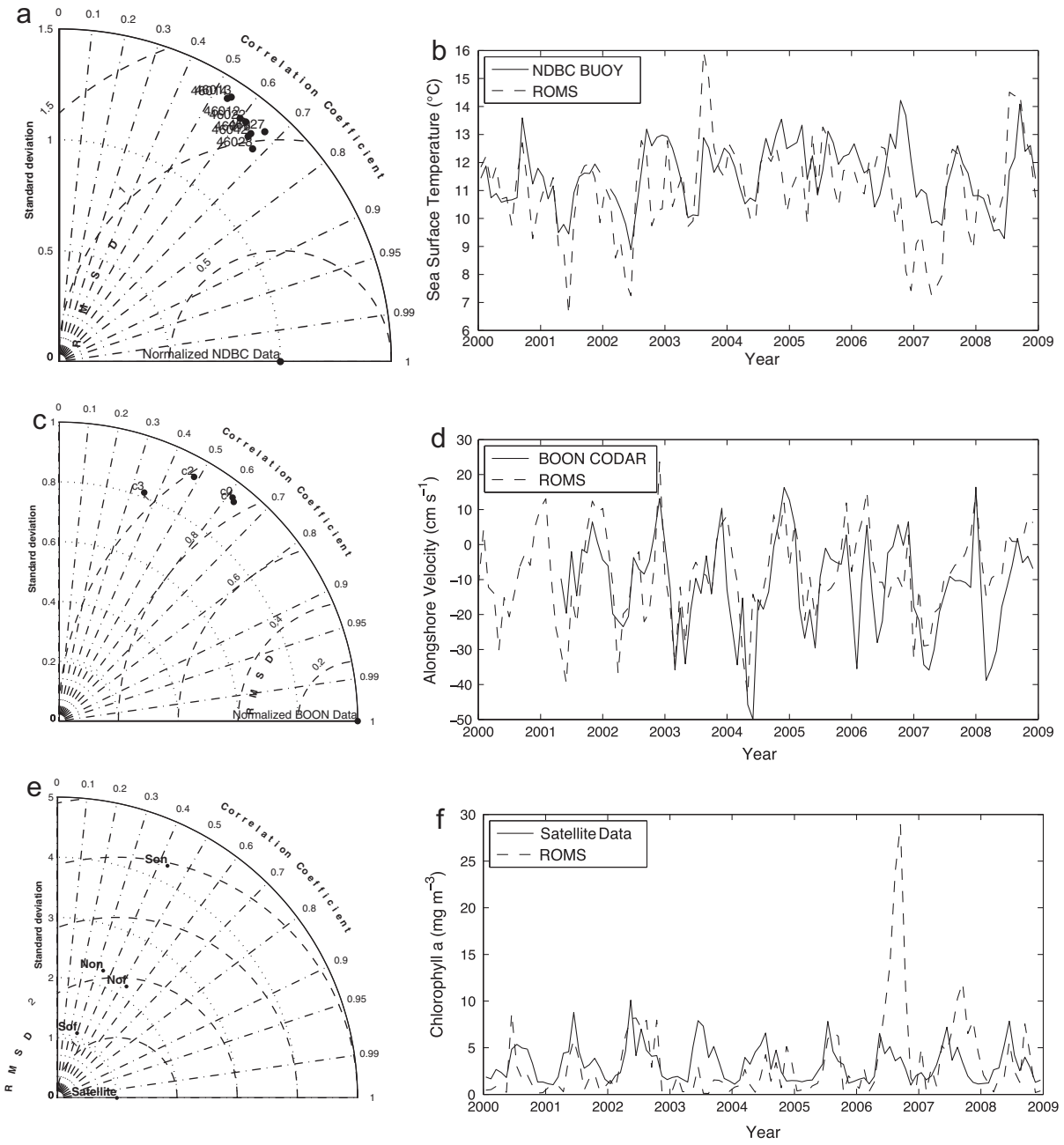

Fig. 7. Taylor diagrams (a, c, e) and time-series (b, d, f) of observed and modeled (a and b) sea surface temperature, (c and d) alongshore-surface currents, and (e and f) chlorophyll *a*. Taylor diagrams display correlation coefficient (curved exterior axis), normalized standard deviation, and root mean squared deviation (curved interior axis). Station locations correspond to (a) NDBC Station ID's, (c) CODAR regions from onshore (c0) to offshore (c3), and (e) north/south, onshore/offshore regions identified in Fig. 2. Time-series data are from (b) NDBC Station 46013, (d) the most inshore CODAR location, and (f) the northern onshore region. All regions are identified in Fig. 1.

(Shaw et al., 2010). Using the conversion from weight to length listed in Appendix A, modeled growth rates of adults at 8 °C and 12 °C and under food unlimited conditions were 0.038 and 0.048 mm d^{-1}, respectively. Under the same conditions, mean growth rate of the entire lifespan was 0.044 and 0.060 mm d^{-1}. While modeled adult growth rates are slightly higher than average experimental rates, differences are not substantial and may be explained by the fact that field specimens were not grown under food unlimited conditions (Shaw et al., 2009).

Reproduction

Experimental data on the median inter-brood period (4.5 days) and mean brood size (109 eggs) of *Euphausia pacifica* maintained at 10.5 °C under food unlimited conditions (Feinberg et al., 2007) is similar to modeled results (IBP = 6.5 days, brood size = 130 eggs) derived under similar conditions (temperature, food conditions, and organism size (20 mm or ~4400 μg C)). These results also are well within the range of reported values from other studies (Ross et al., 1982; Pinchuk and Hopcroft, 2006).

Mortality

Krill can adapt to unfavorable conditions through shrinkage in body weight (Marinovic and Mangel, 1999), and this response has been integrated into our model. The ratio of respiration to ingestion provides a baseline upon which to define the food concentrations at which respiration costs outpace ingestion (see

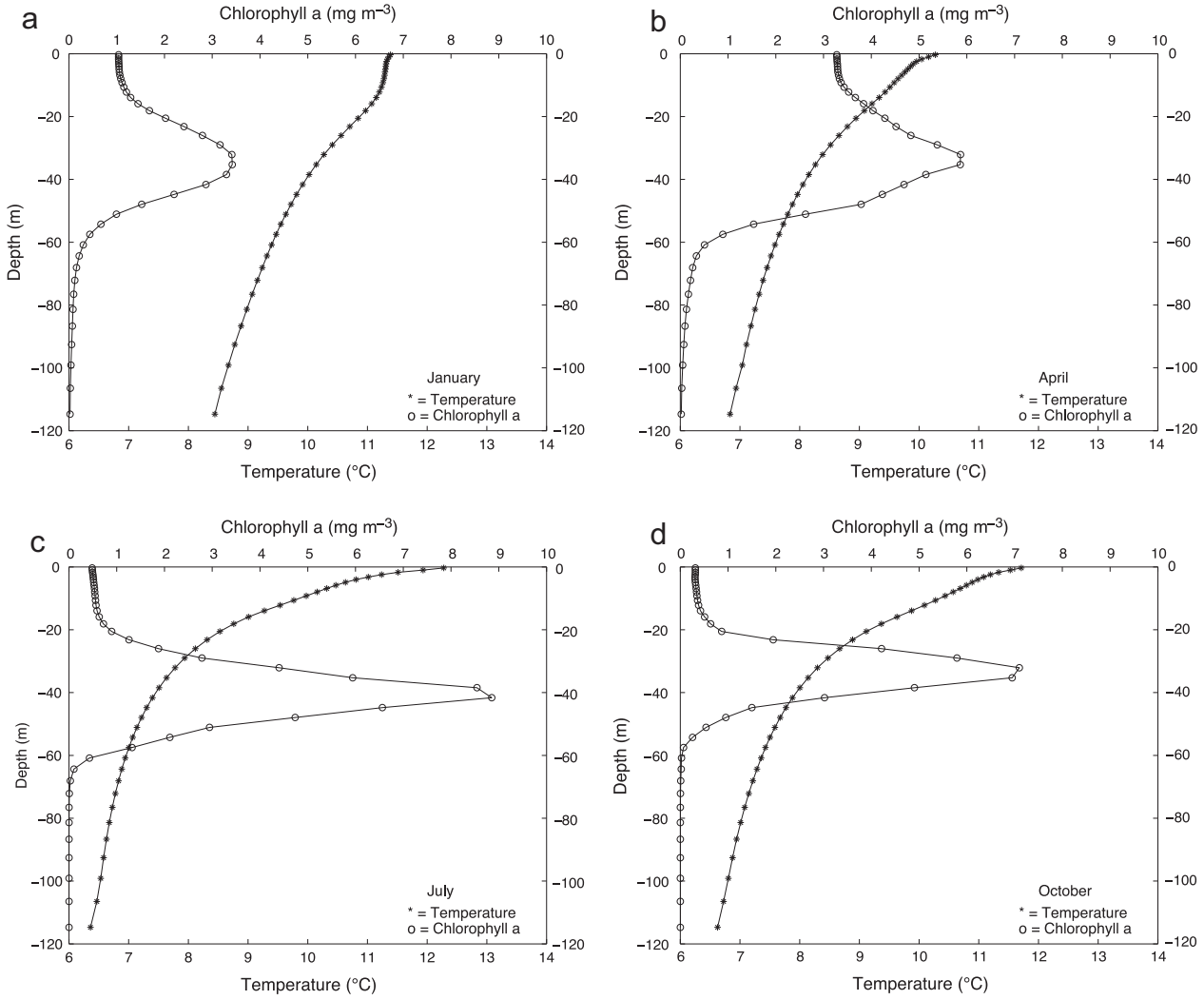

Fig. 8. Average monthly temperature and chlorophyll a vertical profiles from 38.24 N latitude, 123.30 W longitude (location of National Data Buoy Center Station 46013). Averages taken from data from 2000 to 2008.

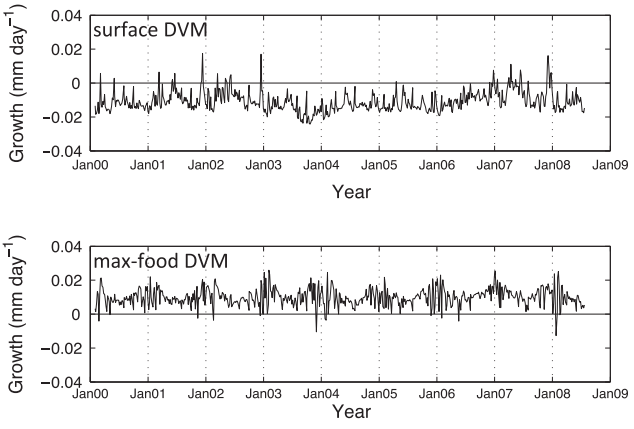

Fig. 9. Average growth rates of *Euphausia pacifica* from the southern onshore analysis region (see Fig. 2). Data are from model runs with the upper limit of diel vertical migration set to (a) 0–10 m (surface DVM) and (b) the depth of maximum chlorophyll *a* (maximum-food DVM). All individual growth rates from the analysis region were averaged together for each saved interval (every 5 days) of the IBM.

Methods). Food concentrations below this level result in negative growth and the beginning of the starvation process. The point at which *Euphausia pacifica* starves has not been empirically determined. Experimental work has shown negative growth in juvenile *E. pacifica* at temperatures higher than 16.5 °C (under food unlimited conditions, Marinovic and Mangel, 1999), but no information is available on the impacts of a lack of food on *E. pacifica* adults. Starvation parameters used within the model are derived from laboratory studies on the Antarctic euphausiid *Euphausia superba*. Krill starvation studies on the first feeding stage of *E. superba* have found a 44–51% loss in body carbon over 10–14 days resulted in the organism reaching a mortality threshold, defined as the point at which an organism cannot recover from starvation even if food conditions improve (Ross and Quetin, 1989). Another study on later furcilia stages determined *E. superba* furcilia IV larvae reach this threshold in 6–9 days and lose approximately 50% of their body carbon (Meyer and Oettl, 2005). Starvation studies on decapod zoea larvae determined that a reduction of body carbon by as little as 20% can result in half of the experimental larvae unable to recover, with an average amount of carbon loss in the 25–35% range (Anger and Dawirs, 1981).

We chose a 30% loss in body carbon to represent a starvation point for our model, as *Euphausia pacifica*, which lives in a food rich environment, is likely less resistant to starvation than *Euphausia superba* which is adapted to overwinter under food-limited conditions. This number is similar to other crustacean larvae threshold values of 20–35% of body carbon loss (Anger and Dawirs, 1981,

1982; Dawirs, 1983). The resultant starvation times of *E. pacifica* larvae are generally in line with reported time to starvation of *E. superba* larvae. Adult starvation times are likely a bit too long under colder conditions, but values in the 100–200 day range agree with reports of *E. superba* adults surviving for over 200 days without food (Ikeda and Dixon, 1982).

Modeling under variable ocean conditions

Only growth, reproduction, and mortality was examined using the model integrated with ROMS as all particles were initiated as adults.

Growth

Growth results from the model integrated with ROMS (i.e., realistic ocean conditions) agree with field data (Shaw et al., 2010, average rate = 0.01 mm d^{-1}), but only in our maximum-food DVM model runs. Migrating the organisms to the maximum food levels as opposed to surface waters is consistent with the purpose of a nighttime ascent to feed in the more productive upper water. In these cases it also limited exposure to warmer surface waters (which increase respiratory costs), especially during summer when offshore surface temperatures can be quite high in comparison with the coastal upwelling region.

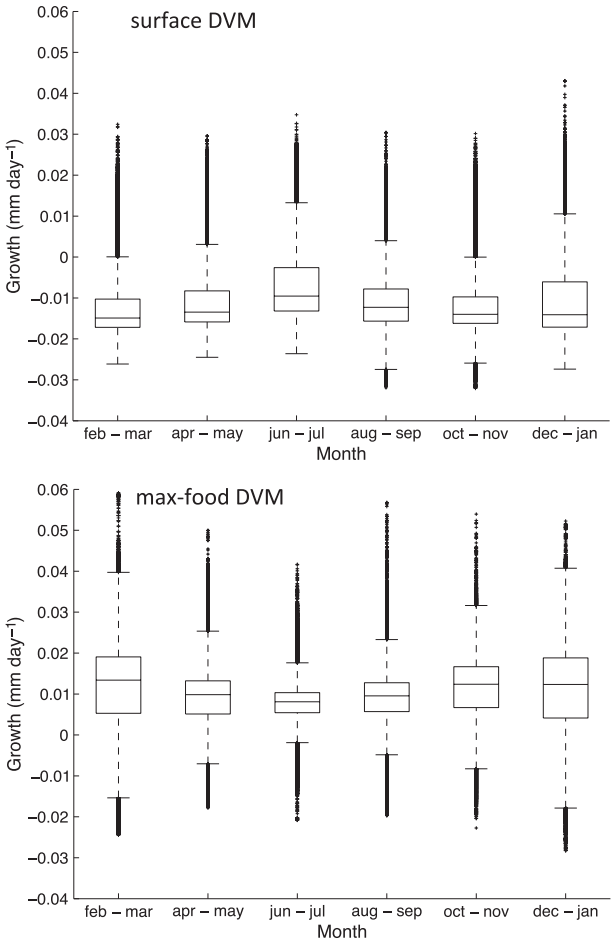

Fig. 10. Average growth rates of *Euphausia pacifica* from the southern onshore analysis region (see Fig. 2). Data are from model runs with the upper limit of diel vertical migration set to (a) 0–10 m (surface DVM) and (b) the depth of maximum chlorophyll *a* (maximum-food DVM). Boxplots display median, limits of 25th and 75th percentile, range of data (whiskers) and outliers. All individual growth rates from the southern onshore analysis region and during displayed 2-month interval (from all years 2000–2008) were used to create the box-plot.

The average rate of adult growth in our model is very slow (3.65 mm $year^{-1}$), considering that the lifespan of these organisms is likely no more than two years in colder waters (i.e., Oregon coast) and as short as 8 months in warmer Californian waters (Brinton, 1976). While average field growth rates agree with our results, field growth rates have a higher upper range (Shaw et al., 2010; Smiles and Pearcy, 1971) than realized in our model. We believe that our phytoplankton results represent the general trends and magnitude of phytoplankton abundance in the central-northern California Current and that the parameterization of bioenergetics is accurate and based on the best available data. The models potential underestimation of growth provides insight

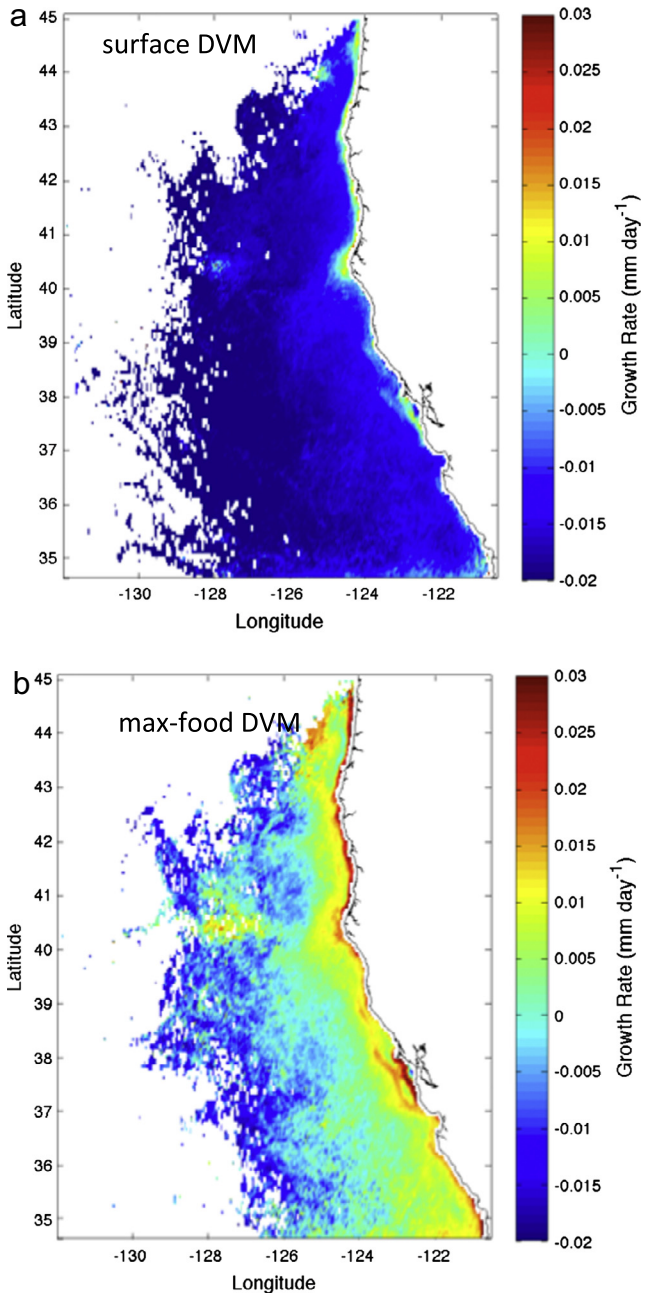

Fig. 11. Average growth rates of *Euphausia pacifica* in April-May from 2000 to 2008, with the upper limit of diel vertical migration set to (a) 0–10 m (surface DVM) and (b) the depth of maximum chlorophyll *a* (maximum-food DVM). All individual growth rates from within each ROMS grid cell were averaged from all model runs during April and May of 2000–2008.

into other factors that might be influencing higher growth rates in the field.

In order to simplify our model we have only allowed *Euphausia pacifica* to feed on phytoplankton which may have resulted in an underestimation of their food intake. *E. pacifica* are omnivorous and opportunistic feeders and can utilize small zooplankton (Lasker, 1966; Ohman, 1984), marine snow (Dilling et al., 1998), and protists (Nakagawa et al., 2004) as food sources. Less is known of the impact of these other prey items on bioenergetics of *E. pacifica* compared to phytoplankton, although small copepods have been shown to meet respiratory costs of *E. pacifica* (Ohman, 1984). As a vertically migrating organism, the *E. pacifica* population spends approximately half of its time at depth (>100 m) in phytoplankton-devoid waters. This results in a loss of weight due to respiration costs in our model runs and opportunistic feeding on available food resources at depth could reduce or eliminate negative growth rates in the model. Under the assumption that *E. pacifica* can meet respiration costs by feeding on non-phytoplankton resources, we ran an additional suite of 60-day model runs beginning on April 1 for the years 2000–2008 where weight loss due to low food resources was eliminated. Resultant growth rates were greater than 0.02 mm d^{-1} over the continental shelf and greater than 0.05 mm d^{-1} in a very narrow region along the shoreline (Dorman et al., unpublished data). This is an approximate doubling of growth rate, compared with previous runs, and is more closely in line with field data. Our simplified prey field is instructive

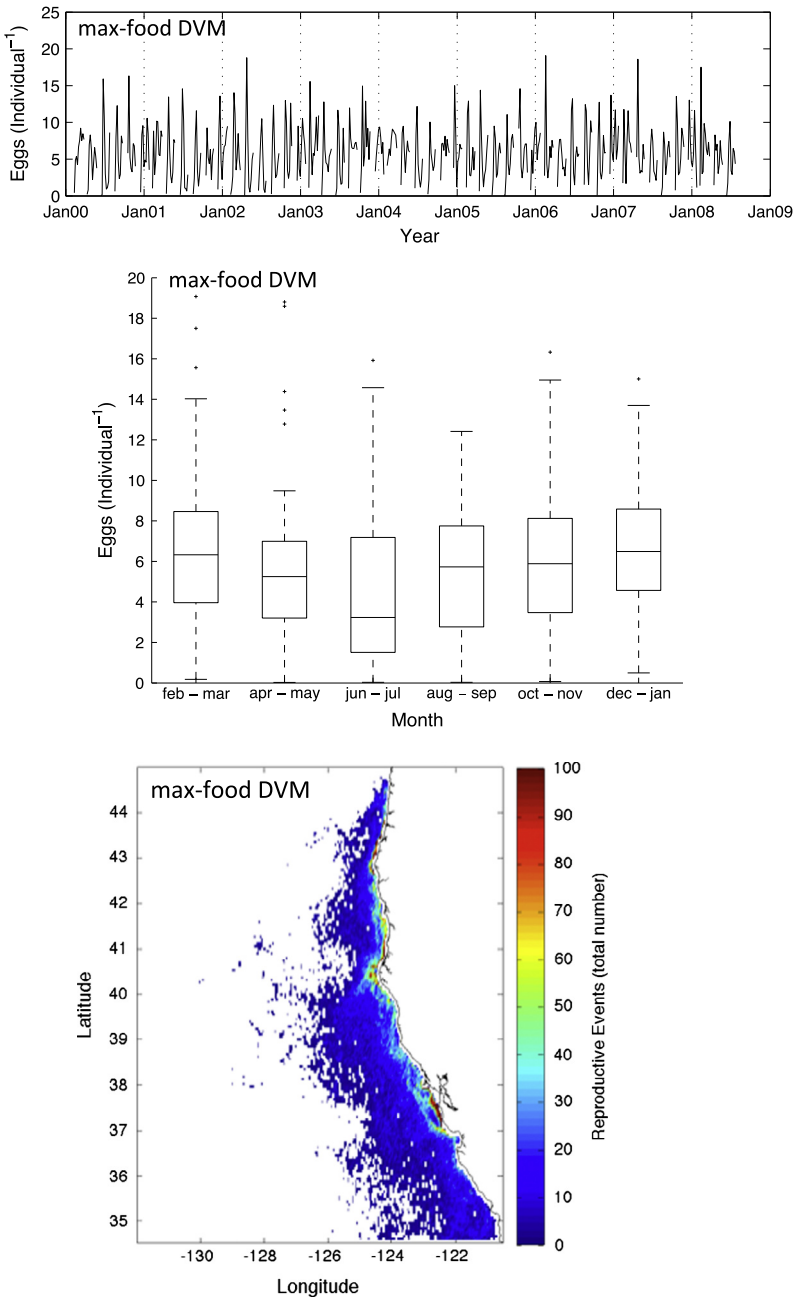

Fig. 12. (a) Average number of eggs released per female *Euphausia pacifica*. Average is from all individuals in the southern onshore analysis region (Fig. 2) for each saved interval (every 5 days) of the IBM. (b) Number of eggs released per female *Euphausia pacifica* from 2000 to 2008, binned into 2-month intervals from the southern onshore analysis region (see Fig. 2). Boxplots display median, limits of 25th and 75th percentile, range of data (whiskers) and outliers. The average calculated for Fig. 12a is the data used to create the boxplots. (c) Total number of reproductive events in April-May from 2000 to 2008.

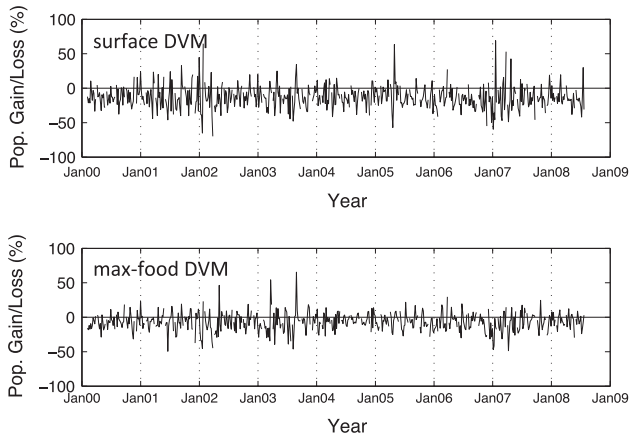

Fig. 13. Population gain/loss as a percentage of the population of *Euphausia pacifica* from the southern onshore analysis region (see Fig. 2) from model runs with the upper limit of diel vertical migration set to (a) 0–10 m (surface DVM) and (b) the depth of maximum chlorophyll *a* (maximum-food DVM). Population gain/loss was calculated for the southern onshore analysis region for each saved interval (every 5 days) of the IBM.

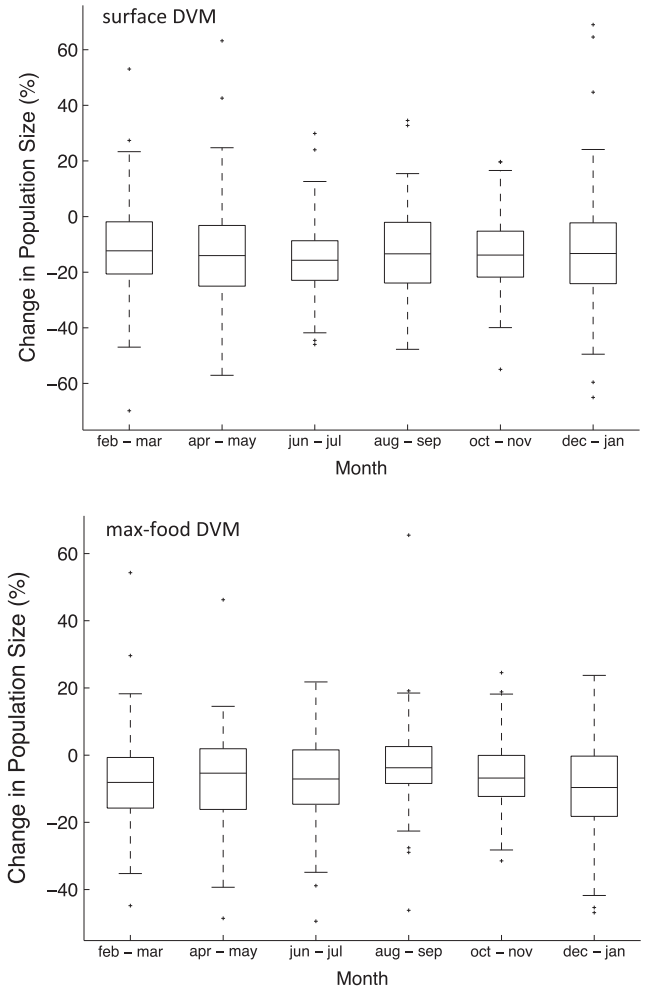

Fig. 14. Population gain/loss as a percentage of the population of *Euphausia pacifica* from the southern onshore analysis region (see Fig. 2). Data are from model runs with the upper limit of diel vertical migration set to (a) 0–10 m (surface DVM) and (b) the depth of maximum chlorophyll *a* (maximum-food DVM). Boxplots display median, limits of 25th and 75th percentile, range of data (whiskers) and outliers. Population gain/loss values measured within each 2-month interval (from all years 2000–2008) were used to create the box-plot.

as a first cut at modeling this important species, but future modeling efforts should consider multiple food resources for *E. pacifica*.

The results of our model also highlight the importance of cross-shelf position on population growth. Higher growth rates are observed year-round over the continental shelf (0.03 mm d^{-1}), which would allow adults to grow approximately 10 mm $year^{-1}$

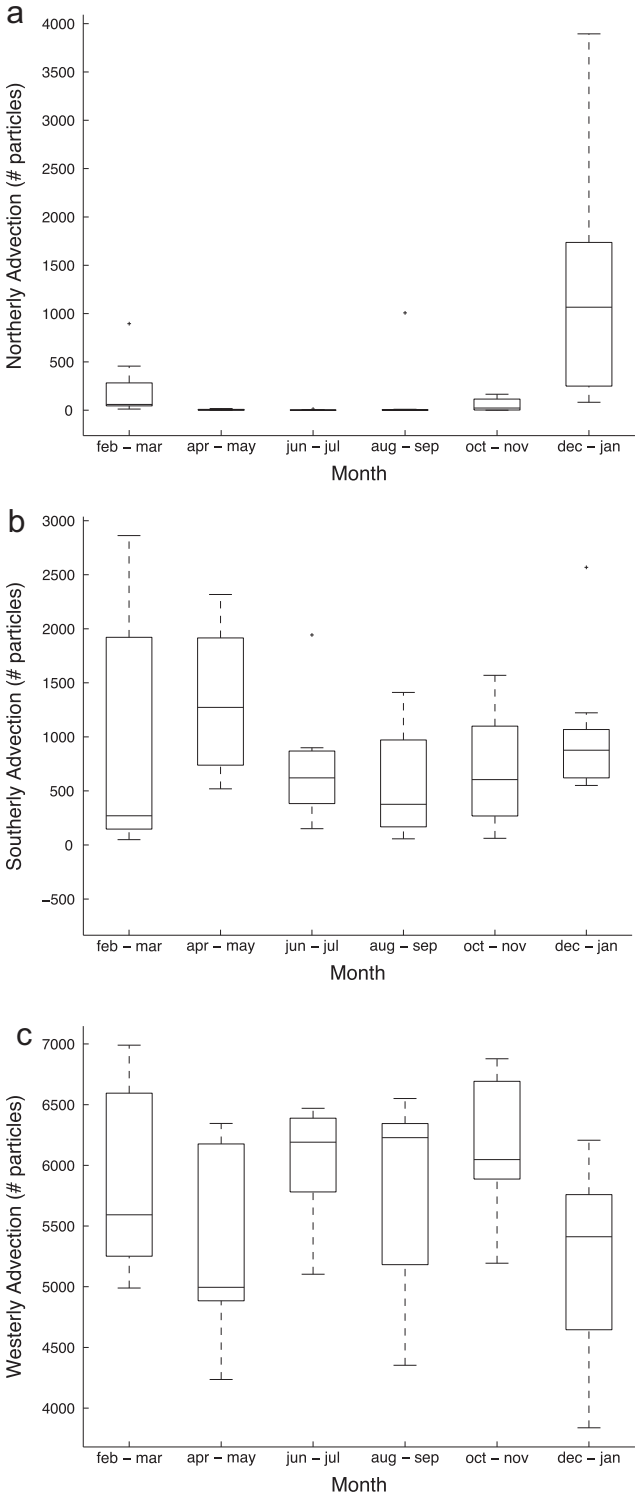

Fig. 15. Particles transported (a) beyond the northern model boundary, (b) beyond the southern model boundary, and (c) beyond 100 km offshore (westward). Boxplots display median, limits of 25th and 75th percentile, range of data (whiskers) and outliers. Number of particles was measured at the end of each 60-day model run (from all years 2000–2008).

feeding strictly on phytoplankton (Fig. 11). Vertical migration into an onshore flowing bottom boundary layer during upwelling events has been shown to enhance shelf retention among modeled zooplankton (Batchelder et al., 2002) and field observations of nearshore spawning events of *Euphausia pacifica* have also been linked to onshore flows during upwelling events (Feinberg and Peterson, 2003). There is also distinct cross-shelf zonation observed in euphausiid species in the California Current (Brinton, 1962; Dorman et al., 2005; Gómez-Gutiérrez et al., 2005) and hotspots of krill (from acoustic data) have been repeatedly observed along the shelf-break (Santora et al., 2011), perhaps indicating active population maintenance strategies. While some of our modeled particles remain entrained inshore, many are advected offshore over the course of a 60-day model run as well (Fig. 15). The vertical migratory behavior in our model does not incorporate any strategies designed to maintain the population onshore in response to cues from currents or variability in shear that might aid in retention over the shelf, as our knowledge of any such behaviors is not known. These results highlight the importance of maintaining a nearshore position to achieve growth rates in line with the upper limit of field observations.

Other factors that occur on a smaller spatial scale than our model can identify have the potential to increase growth rates in field populations. Turbulence has been shown to increase predator–prey interaction (Werner et al., 1996) by increasing the encounter rate of predators with their prey. Prey patches, which often occur at the sub kilometer scale, have been shown to be critically important for increasing predator feeding efficiency (Benoit-Bird et al., 2013). Neither of these processes are represented in our model and may also be important in growth of the *Euphausia pacifica* population in the field.

Reproduction

Reproduction results integrated with the ROMS model exhibit consistent year-round reproduction throughout the model domain. Year-round reproduction has been reported off southern (Brinton, 1976) and northern California (Dorman et al., 2005), but in colder regions of the California Current (Oregon, Washington), seasonal reproduction occurs synchronized with high primary productivity (Feinberg and Peterson, 2003). Our IBM allocates energy to reproduction whenever growth is positive, thus our model exhibits year-round reproduction in these regions. More northern populations of *Euphausia pacifica* may be exhibiting alternative reproductive strategies regarding energy allocation during less productive seasons (Hagen, 1999). These types of strategies (e.g., lipid accumulation) are common among krill species in colder regions and will need to be incorporated into future versions of the model to accurately represent spatial heterogeneity in the population biology of *E. pacifica*.

Mortality

Model runs integrated with ROMS resulted in no starvation. Preliminary model runs of adult krill that were extended from a 60 days run to 180 days resulted in very few instances of starvation. Considering the omnivorous nature of *Euphausia pacifica*, these results jibe with our understanding of their population biology. Preliminary runs where initial particles were seeded as eggs resulted in considerable starvation, often greater than 50% of the population. Larval *E. pacifica* have much smaller reserve energy resources and are weak vertical migrators, thus unable to initiate and maintain contact with high food concentrations. While preliminary, these results indicate a potential source of mortality that might occur due to event-scale (weekly) poor food conditions in the California Current.

There is very little knowledge on the physiological response of *Euphausia pacifica* to food limited conditions and starvation results from the model should be considered with a critical eye. Further experimental work on starvation and feeding under low levels of food would be very useful for future modeling efforts and in understanding ocean conditions that might lead to poor survival of *E. pacifica* in the California Current.

Temporal variability

Interannual variability

Our analysis for interannual variability in growth rates of *E. pacifica* from 2000 to 2008 showed little year-to-year differences in growth rate, reproduction, and retention, despite known interannual variation in krill abundance in the central California region (Sydeman et al., 2006; Lindley et al., 2009). This discrepancy may, at least in part, be due to comparing different data products: abundance (from field sampling of krill) and growth, reproduction, and retention (from our model). Our model measurements ultimately influence the abundance of krill, but over varying integrated time-periods. Advection would have a short-time scale impact on abundance, while increased periods of reproduction would take at least 3–4 months to be measured as changes in adult abundance in the system. To realize these sorts of results in our model we would have had to run it in such a way to incorporate "biological memory" into our simulations. We chose a more simple methodology, resetting to initial conditions every 2 months, to allow for more clear analysis of our results. Future model runs are planned to explore the importance time-scales of the biological memory of krill in the California Current ecosystem.

Our decision to migrate organisms to the depth of maximum chlorophyll *a* also reduces the variability that is observed due to upwelling events. A visual comparison of Fig. 9a and b shows much more year-to-year consistency in growth rates in our maximum-food DVM model runs. The deep-chlorophyll maximum was present year round in our model (Fig. 8) providing a consistent food resource regardless of food availability in the upper water column. Neither of our modeled vertical migration schemes is "correct" as the upper limit of DVM is highly variable in nature, typically resulting in a diffuse population in the upper part of the water column. Prescribing a set depth to the extent of DVM reduces the number of variables to consider in model analysis, but perhaps influences the amount of natural variability in natural populations.

It should also be noted that much of the interannual variability ("good" or "bad" years) in krill abundance in the central California Current, often reflect the state of krill during the upwelling season, as that is when the majority of the sampling takes place (Dorman et al., 2005; Sydeman et al., 2006; Santora et al., 2011). Our interest in krill relates to their impact on predators who may have temporally small windows (month long) for critical life-stage (often juvenile feeding stages) development. Thus a seasonal decline in krill availability, as was observed in the central California Current in early 2005 (a "bad-year"), can have large impacts (on the annual scale) on predators (Sydeman et al., 2006; Lindley et al., 2009). The annual integrated effect of upwelling on primary production (and presumably krill) over the entire year of 2005 was ultimately fairly normal (Thomas and Brickley, 2006). The ability to average an entire years worth of model data may actually smooth over the variability that is observed in the California Current on a seasonal or shorter-time scale. These results may be a more accurate representation of the variability in modeled krill on an interannual basis than temporally-biased field sampling.

Seasonal variability

The most apparent seasonal signal observed is higher variability in growth rates during the winter months of the maximum-food DVM model runs (Figs. 9 and 10). As growth is partially dependent on food resources and the individuals are migrating up to the

depth of maximum food, the result indicates that some of the most and least productive conditions are during the winter. Upwelling in the lower latitudes of the California Current region exhibits a seasonal cycle, but episodic upwelling events occur with some regularity during the "non-upwelling" season (Bograd et al., 2009). Growth rates during productive periods in winter are likely enhanced by the cooler temperatures which reduce overall metabolic costs. It has been suggested that favorable winter conditions in the California Current "pre-condition" the biological system for a productive spring/summer season (Schroeder et al., 2009, 2013; Black et al., 2010). These results suggest there is the potential for prolonged periods of greater growth of *E. pacifica* during winter. These conditions would produce larger adults during the spring, leading to greater reproductive potential, and provide greater food resources to higher trophic levels during the upwelling season.

There is a surprising lack of a seasonal signal in the particle retention data. We expected greater loss of particles from our analysis regions during the traditional upwelling season as surface waters are transported offshore. The lack of seasonal signal is likely due to the replacement of particles that are lost offshore during upwelling by particles from regions to the north or south of our analysis region. This may be partially an artifact of our model initial conditions, which spaced our krill particles evenly along the coastline. Acoustic records show significant alongshore variability in krill abundance along the coast (Santora et al., 2011) and regions of high or low abundance adjacent to our analysis regions could certainly impact local abundance. An analysis of the particle retention of only those individuals that were initialized in our analysis region does exhibit a seasonal signal with 0–10% of particles remaining after 2 months during upwelling season (March–June) and upwards of 35% of the particles remaining during fall/winter months (October–December) (data not shown). It is unclear whether advective losses of this nature would be detrimental to population maintenance. It is assumed that diel vertical migration aids in shelf retention of zooplankton, or at a minimum, reduces advective losses from the shelf. As we have only seeded migratory adult *Euphausia pacifica* in our model, we would expect greater advective losses in non-migratory calyptopis and weakly migratory furcilia life stages.

Event scale variability

Event scale dynamics have been shown to be important in understanding phytoplankton and zooplankton abundance along the Northern California coast (Largier et al., 2003). Our data suggest that while growth can be greatest under more intense upwelling conditions, these conditions also can lead to a greater loss of particles (Fig. 16) from the coastal environment. The differences we observe in the relationship between growth and upwelling proxies and particle retention and upwelling proxies agrees with the idea of an optimal amount of upwelling for planktonic organisms (Cury and Roy, 1989; Botsford et al., 2003; García-Reyes et al., 2014). Increases in reproduction did not correspond well with upwelling indicators, likely due to time it takes to convert energy intake into reproductively mature eggs. An organism might

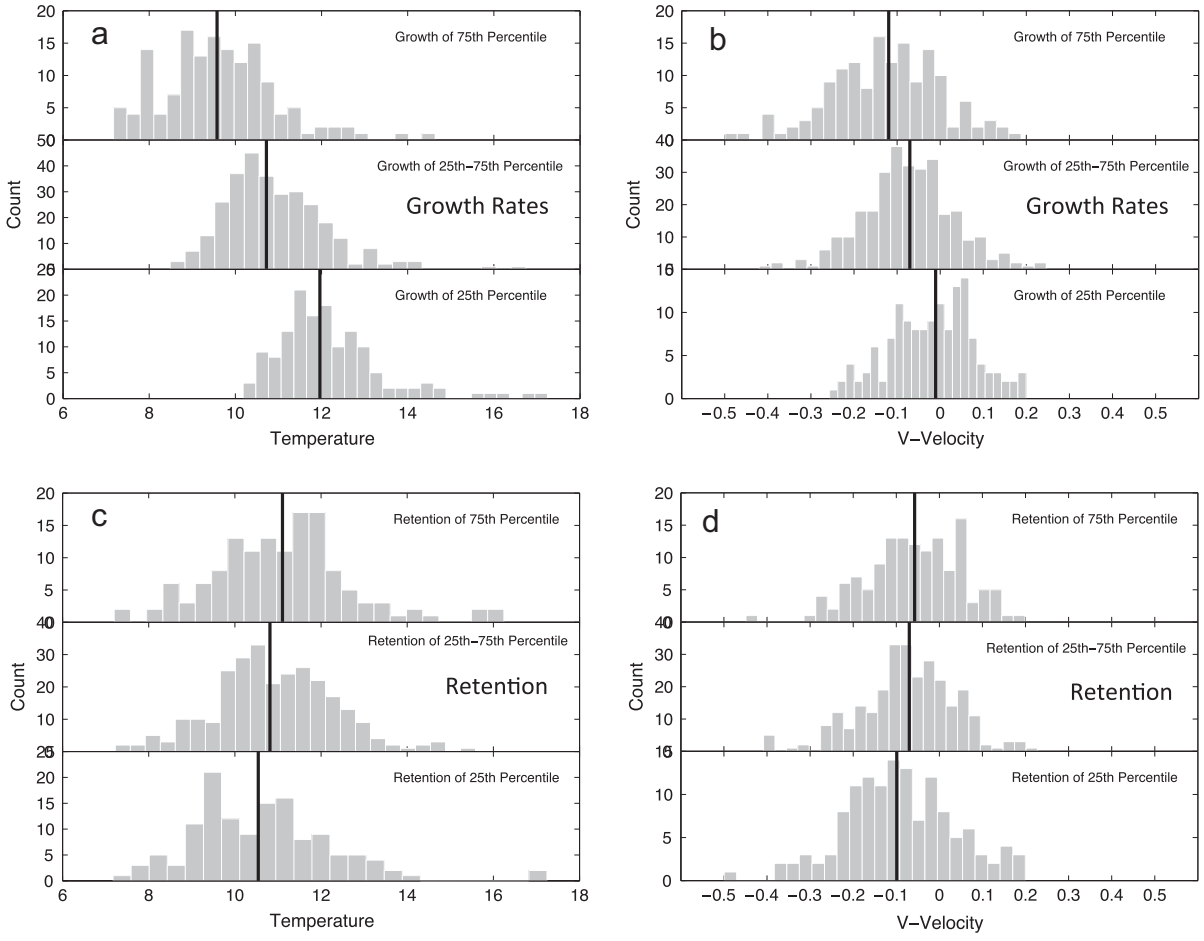

Fig. 16. Histograms comparing average growth rate (a and b) and population retention (c and d) over 5-day intervals to sea surface temperature (a and c) and alongshore-surface current velocity (b and d; negative is equatorward). Each set of three histograms show instances of the upper 25th percentile (upper panel) of growth/retention, the 25th–75th percentile (middle panel) of growth/retention, and the lower 25th percentile (lower panel) of growth/retention. Black vertical lines is the median value of temperature or alongshore current for that group. Average growth rate and population retention data is from the time-series of Figs. 9 and 13, respectively.

increase reproductive potential (i.e., convert a lot of energy to eggs) during upwelling events, but the release of those eggs might be constrained by timing factors that determine interbrood period in our model.

Conclusion

Our integrated, coupled ROMS–IBM provides realistic parameters and output for *Euphausia pacifica*, a key prey species for seabirds, marine mammals and predatory fish in the California Current. Variation in the vertical migration scheme so that particles migrated to the chlorophyll maximum layer has significant effects on individual growth rates. Under this scenario, individuals have positive growth rates throughout the continental shelf and shelf-break region. Moreover, as particles spent less time in the upper 10 m of the water column, advection out of the model domain was also reduced (southward during summer and northward during winter), resulting in a larger and more stable population. Modeled individual growth rates are consistently lower than field measurements, indicating the potential importance of non-phytoplankton food resources, cross-shelf position, and smaller-scale processes for the survival and reproduction *E. pacifica*. Our model provides a new tool for the ecosystem approach to fisheries in the California Current and possibly elsewhere in the world where *E. pacifica* are key in coastal food webs and predator–prey interactions. Our IBM for *E. pacifica* could be linked with downscaled global climate models to understand and provide outlooks for these populations under changing climate and oceans.

Acknowledgements

We gratefully thank the many communities that provide data to make a modeling project such as this possible: National Centers for Environmental Prediction, Asia–Pacific Data Research Center, National Oceanographic Data Center, NOAA-National Data Buoy Center, Bodega Ocean Observing Node, NASA-Goddard Space Flight Center. Model development by the ROMS community and by Dr. Hal Batchelder have also been instrumental in this work. This research was supported by California Sea Grant Project R/OPCENV-07 and Project R/ENV-220.

Appendix A

Scaling and conversion equations

Temperature scaling of multiple model parameters (P) was achieved using Q_{10} values as shown in Eq. (A.1) where P_T = temperature adjusted parameter, T = model temperature, and T_{Q10} = the temperature at which the experimental work was conducted to determine model parameters.

$$P_T = PQ_{10}^{\left(\frac{T-T_{Q10}}{10}\right)} \tag{A.1}$$

Phytoplankton concentration from ROMS is output in units of μmol Nitrogen l^{-1} and is converted to units of μg Carbon l^{-1} for use in the IBM, and to units of cells ml^{-1} for use in an experimentally derived ingestion equation (Ohman, 1984). ROMS phytoplankton output is converted to units of μg carbon with Eq. (A.2), using the Redfield ratio of carbon to nitrogen (106:16) and the atomic weight of carbon (~12) to calculate a ratio of 77 μg carbon: 1 μmol nitrogen.

$$\left(\frac{106\ \mu\text{mol C}}{16\ \mu\text{mol N}}\right)\left(\frac{12\ \mu\text{g N}}{1\ \mu\text{mol C}}\right) \approx \left(\frac{77\ \mu\text{g C}}{1\ \mu\text{mol N}}\right) \tag{A.2}$$

Further conversion of phytoplankton to units used in the ingestion equation (cells ml^{-1}) was based on the reported ingestion rate of 22,950 cells euphausiid^{-1} h^{-1} (90% of the maximum ingestion rate) being equal to 290 μg C l^{-1} (Ohman, 1984).

From these data we can determine the average carbon weight of each cell of the diatom used in the ingestion study (*Thalassiosira angstii*; 661 pg carbon cell^{-1}). Thus, modeled phytoplankton (P_m, μg l^{-1}) is converted to the prey concentration units of this equation (cells ml^{-1}) using Eq. (A.3). This estimate of the phytoplankton carbon cell^{-1} is similar to values for diatoms reported by Strathmann (1967).

$$P_m\left(\frac{\mu\text{g C}}{\text{l}}\right)\left(\frac{10^6\ \text{pg C}}{1\ \mu\text{g C}}\right)\left(\frac{1\ \text{l}}{10\ \text{ml}}\right)\left(\frac{1\ \text{cell}}{661\ \text{pg C}}\right) = \left(\frac{\text{cells}}{\text{ml}}\right) \tag{A.3}$$

Phytoplankton output was further converted to chlorophyll *a* for comparison with observational data using the conversion of 1 μg chlorophyll *a* per 60 μg carbon. There is known variation in the ratio of chlorophyll *a* to carbon (Strickland, 1965; Banse, 1977) with factors such as light, nutrient concentration and temperature all influencing the ratio. The ratio of 1:60 that is used falls within commonly used values for upwelling regions.

To convert model growth rates (μg C d^{-1}) to published growth rates (mm d^{-1}) we assumed that 40% of dry weight of *Euphausia pacifica* is comprised of carbon based on published values between 38.1% and 45.1% (Lasker, 1966; Ross, 1982a; Iguchi and Ikeda, 1999) and used the dry weight to total length relationship published by Feinberg et al. (2007).

References

Anger, K., Dawirs, R., 1981. Influence of starvation on the larval development of *Hyas araneus* (Decopoda, Majidae). Helgoländer Meeresuntersuchungen 34, 287–311.
Anger, K., Dawirs, R., 1982. Elemental composition (C, N, H) and energy in growing and starving larvae of *Hyas araneus* (Decapoda, Majidae). Fishery Bulletin 80, 419–433.
Banse, K., 1977. Determining the carbon-to-chlorophyll ratio of natural phytoplankton. Marine Biology 41, 199–212.
Batchelder, H.P., Miller, C.B., 1989. Life history and population dynamics of *Metridia pacifica*: results from simulation modeling. Ecological Modelling 48, 113–136.
Batchelder, H.P., Powell, T.M., 2002. Physical and biological conditions and processes in the northeast Pacific Ocean. Progress in Oceanography 53, 105–114.
Batchelder, H.P., Edwards, C.A., Powell, T.M., 2002. Individual-based models of copepod populations in coastal upwelling regions: implications of physiologically and environmentally influenced diel vertical migration on demographic success and nearshore retention. Progress in Oceanography 53, 307–333.
Benoit-Bird, K.J., Battaile, B.C., Heppell, S.A., Hoover, B., Irons, D., Jones, N., Kuletz, K.J., Nordstrom, C.A., Paredes, R., Suryan, R.M., Waluk, C.M., Trites, A.W., 2013. Prey patch patterns predict habitat use by top marine predators with diverse foraging strategies. PLoS ONE 8, e53348.
Black, B.A., Schroeder, I.D., Sydeman, W.J., Bograd, S.J., Lawson, P.W., 2010. Wintertime ocean conditions synchronize rockfish growth and seabird reproduction in the central California Current ecosystem. Canadian Journal of Fisheries and Aquatic Sciences 67, 1149–1158.
Bograd, S.J., Schroeder, I., Sarkar, N., Qui, X., Sydeman, W.J., Schwing, F.B., 2009. Phenology of coastal upwelling in the California Current. Geophysical Research Letters 36, L01602.
Bollens, S.M., Frost, B.W., Lin, T.S., 1992. Recruitment, growth, and diel vertical migration of *Euphausia pacifica* in a temperate fjord. Marine Biology 114, 219–228.
Botsford, L.W., Lawrence, C.A., Dever, E.P., Hastings, A., Largier, J., 2003. Wind strength and biological productivity in upwelling systems: an idealized study. Fisheries Oceanography 12, 245–259.
Brinton, E., 1962. The distribution of Pacific euphausiids. Bulletin of the Scripps Institution of Oceanography of the University of California 8, 51–269.
Brinton, E., 1976. Population biology of *Euphausia pacifica* off southern California. Fishery Bulletin 74, 733–762.
Butcher, J.C., 2003. Numerical Methods for Ordinary Differential Equations. John Wiley & Sons, Chichester, West Sussex, England.
Carton, J.A., Giese, B.S., 2008. A reanalysis of ocean climate using Simple Ocean Data Assimilation (SODA). Monthly Weather Review 136, 2999–3017.
Chai, F., Dugdale, R.C., Peng, T.-H., Wilkerson, F.P., Barber, R.T., 2002. One dimensional ecosystem model of the equatorial Pacific upwelling system. Part 1: model development and silicon and nitrogen cycle. Deep-Sea Research II 49, 2713–2745.
Chai, F., Liu, G., Xue, H., Shi, L., Chao, Y., Tseng, C.-T., Chou, W.-C., Liu, K.-K., 2009. Seasonal and interannual variability of carbon cycle in South China Sea: a three-

dimensional physical-biogeochemical modeling study. Journal of Oceanography 65, 703–720.
Checkley Jr., D.M., Barth, J.A., 2009. Patterns and processes in the California Current System. Progress in Oceanography 83, 49–64.
Cury, P., Roy, C., 1989. Optimal environmental window and pelagic fish recruitment success in upwelling areas. Canadian Journal of Fisheries and Aquatic Sciences 46, 670–680.
Dawirs, R., 1983. Respiration, energy balance and development during growth and starvation of *Carcinus maenas* L. larvae (Decapoda: Portunidae). Journal of Experimental Marine Biology and Ecology 69, 105–128.
Di Lorenzo, E., Schneider, N., Cobb, K.M., Franks, P.J.S., Chhak, K., Miller, A.J., McWilliams, J.C., Bograd, S.J., Arango, H., Curchitser, E., Powell, T.M., Riviere, P., 2008. North Pacific Gyre Oscillation links ocean climate and ecosystem change. Geophysical Research Letters 35, L08607.
Dilling, L., Wilson, J., Steinberg, D., Alldredge, A., 1998. Feeding by the euphausiid *Euphausia pacifica* and the copepod *Calanus pacificus* on marine snow. Marine Ecology Progress Series 170, 189–201.
Dorman, J.G., 2011. The Influence of Seasonal and Decadal Trends in Coastal Ocean Processes on the Population Biology of the Krill Species *Euphausia pacifica*: Results of a Coupled Ecosystem and Individual based Modeling Study. Ph.D. Thesis, University of California, Berkeley, unpublished.
Dorman, C.E., Winant, C.D., 1995. Buoy observations of the atmosphere along the west coast of the United States, 1981–1990. Journal of Geophysical Research: Oceans 101, 16029–16044.
Dorman, J.G., Bollens, S.M., Slaughter, A.M., 2005. Population biology of euphausiids off northern California and effects of short time-scale wind events on *Euphausia pacifica*. Marine Ecology Progress Series 288, 183–198.
Edwards, A.M., Yool, A., 2000. The role of higher predation in plankton population models. Journal of Plankton Research 22, 1085–1112.
Fairall, C.W., Bradley, E.F., Rogers, D.P., Edson, J.B., Young, G.S., 1996. Bulk parameterization of air-sea fluxes for Tropical Ocean-Global Atmosphere Coupled-Ocean Atmosphere Response Experiment. Journal of Geophysical Research 101 (C2), 3747–3764.
Feinberg, L.R., Peterson, W.T., 2003. Variability in duration and intensity of euphausiid spawning off central Oregon, 1996–2001. Progress in Oceanography 57, 363–379.
Feinberg, L.R., Shaw, C.T., Peterson, W.T., 2006. Larval development of *Euphausia pacifica* in the laboratory: variability in the developmental pathways. Marine Ecology Progress Series 316, 127–137.
Feinberg, L.R., Shaw, C.T., Peterson, W.T., 2007. Long-term laboratory observations of *Euphausia pacifica* fecundity: comparison of two geographic regions. Marine Ecology Progress Series 341, 141–152.
Field, J.C., Francis, R.C., 2006. Considering ecosystem-based fisheries management in the California current. Marine Policy 30, 552–569.
Field, J.C., Francis, R.C., Aydin, K., 2006. Top-down modeling and bottom-up dynamics: linking a fisheries-based ecosystem model with climate hypotheses in the Northern California Current. Progress in Oceanography 68, 238–270.
García-Reyes, M., Largier, J.L., Sydeman, W.J., 2014. Synoptic-scale upwelling indices and predictions of phyto- and zooplankton populations. Progress in Oceanography 120, 177–188.
Gillooly, J.F., Brown, J.H., West, G.B., Savage, V.M., Charnov, E.L., 2001. Effects of size and temperature on metabolic rate. Science 293, 2248–2251.
Gómez-Gutiérrez, J., Peterson, W.T., Miller, C.B., 2005. Cross-shelf life-stage segregation and community structure of the euphausiids off central Oregon (1970–1972). Deep-Sea Research II 52, 289–315.
Gómez-Gutiérrez, J., Feinberg, L.R., Shaw, T., Peterson, W., 2006. Variability in brood size and female length of *Euphausia pacifica* among three populations in the North Pacific. Marine Ecology Progress Series 323, 185–194.
Gómez-Gutiérrez, J., Feinberg, L.R., Shaw, T., Peterson, W., 2007. Interannual and geographical variability of the brood size of the euphausiids *Euphausia pacifica* and *Thysanoessa spinifera* along the Oregon coast (1999–2004). Deep-Sea Research I 54, 2145–2169.
Hagen, W., 1999. Reproductive strategies and energetic adaptations of polar zooplankton. Invertebrate Reproduction & Development 36, 25–34.
Haidvogel, D.B., Arango, H., Budgell, W.P., Cornuelle, B.D., Curchitser, E., Di Lorenzo, E., Fennel, K., Geyer, W.R., Hermann, A.J., Lanerolle, L., Levin, J., McWilliams, J.C., Miller, A.J., Moore, A.M., Powell, T.M., Shchepetkin, A.F., Sherwood, C.R., Signell, R.P., Warner, J.C., Wilkin, J., 2008. Ocean forecasting in terrain-following coordinates: Formulation and skill assessment of the Regional Ocean Modeling System. Journal of Computational Physics 227, 3595–3624.
Iguchi, N., Ikeda, T., 1999. Production, metabolism and P: B ratio of *Euphausia pacifica* (Crustacea: Euphausiacea) in Toyama Bay, southern Japan Sea. Plankton Biology and Ecology 46, 68–74.
Ikeda, T., Dixon, P., 1982. Body shrinkage as a possible over-wintering mechanism of the Antarctic krill, *Euphausia superba* Dana. Journal of Experimental Marine Biology and Ecology 62, 143–151.
Kahru, M., Kudela, R.M., Manzano-Sarabia, M., Mitchell, B.G., 2009. Trends in primary productivity in the California Current detected with satellite data. Geophysical Research Letters 114, C02004.
Kishi, M.J., Kashiwai, M., Ware, D.M., Megrey, B.A., Eslinger, D.L., Werner, F.E., Noguchi-Aita, M., Azumaya, T., Fujii, M., Hashimoto, S., Huang, D., Iizumi, H., Ishida, Y., Kang, S., Kantakov, G.A., Kim, H., Komatsu, K., Navrotsky, V.V., Smith, S.L., Tadokoro, K., Tsuda, A., Yamamura, O., Yamanaka, Y., Yokouchi, K., Yoshie, N., Zhang, J., Zuenko, Y.I., Zvalinsky, V.I., 2007. NEMURO-a lower trophic level model for the North Pacific marine ecosystem. Ecological Modelling 202, 12–25.
Largier, J.L., Lawrence, C.A., Roughan, M., Kaplan, D.M., Dever, E.P., Dorman, C.E., Kudela, R.M., Bollens, S.M., Wilkerson, F.P., Dugdale, R.C., Botsford, W.L., Garfield, N., Kuebel Cervantes, B., Koračin, D., 2003. WEST: a northern California study of the role of wind-driven transport in the productivity of coastal plankton communities. Deep-Sea Research II 53, 2833–2849.
Lasker, R., 1966. Feeding, growth, respiration and carbon utilization of a euphausiid crustacean. Journal of the Fisheries Research Board of Canada 23, 1291–1317.
Lindley, S.T., Grimes, C.B., Mohr, M.S., Peterson, W., Stein, J., Anderson, J.T., Botsford, L.W., Bottom, D.L., Busack, C.A., Collier, T.K., Ferguson, J., Garza, J.C., Grover, A.M., Hankin, D.G., Kope, R.G., Lawson. P.W., Low, A., MacFarlane, R.B., Moore, K., Palmer-Zwahlen, M., Schwing, F.B., Smith, J., Tracy, C., Webb, R., Wells, B.K., Williams, T.H., 2009.What Caused the Sacramento River Fall Chinook Stock Collapse? Report to the Pacific Fishery Management Council.
Marinovic, B., Mangel, M., 1999. Krill can shrink as an ecological adaptation to temporarily unfavourable environments. Ecology Letters 2, 338–343.
Meyer, B., Oettl, B., 2005. Effects of short-term starvation on composition and metabolism of larval Antarctic krill *Euphausia superba*. Marine Ecology Progress Series 292, 263–270.
Nakagawa, Y., Ota, T., Endo, Y., Taki, K., Sugisaki, H., 2004. Importance of ciliates as prey of the euphausiid *Euphausia pacifica* in the NW North Pacific. Marine Ecology Progress Series 271, 261–266.
Ohman, M.D., 1984. Omnivory by *Euphausia pacifica*: the role of copepod prey. Marine Ecology Progress Series 19, 125–131.
Pinchuk, A.I., Hopcroft, R.R., 2006. Seasonal variations in the growth rates of euphausiids (*Thysanoessa inermis*, *T. spinifera*, and *Euphausia pacifica*) from the northern Gulf of Alaska. Marine Biology 151, 257–269.
Powell, T.M., Lewis, C.V.W., Curchitser, E.N., Haidvogel, D.B., Hermann, A.J., Dobbins, E.L., 2006. Results from a three-dimensional, nested biological-physical model of the California Current System and comparisons with statistics from satellite imagery. Journal of Geophysical Research 111, C07018.
Ross, R.M., 1979. Carbon and Nitrogen Budgets over the Life of *Euphausia pacifica*. Ph.D. Thesis, University of Washington, Seattle, WA, 260 p.
Ross, R.M., 1981. Laboratory culture and development of *Euphausia pacifica*. Limnology and Oceanography 26, 235–246.
Ross, R.M., 1982a. Energetics of *Euphausia pacifica*. I. Effects of body carbon and nitrogen and temperature on measured and predicted production. Marine Biology 68, 1–13.
Ross, R.M., 1982b. Energetics of *Euphausia pacifica*. II. Complete carbon and nitrogen budgets at 8° and 12 °C throughout the life span. Marine Biology 68, 15–23.
Ross, R.M., Quetin, L.B., 1989. Energetic cost to develop to the first feeding stage of *Euphausia superba* Dana and the effect of delays in food availability. Journal of Experimental Marine Biology and Ecology 133, 103–127.
Ross, R.M., Daly, K.L., Saunders English, T., 1982. Reproductive cycle and fecundity of *Euphausia pacifica* in Puget Sound, Washington. Limnology and Oceanography 27, 304–314.
Santora, J.A., Sydeman, W.J., Schroeder, I.D., Wells, B.K., Field, J.C., 2011. Mesoscale structure and oceanographic determinants of krill hotspots in the California Current: Implications for trophic transfer and conservation. Progress in Oceanography 91, 397–409.
Schroeder, I.D., Sydeman, W.J., Sarkar, N., Thompson, S.A., Bograd, S.J., Schwing, F.B., 2009. Winter pre-conditioning of seabird phenology in the California Current. Marine Ecology Progress Series 393, 211–223.
Schroeder, I.D., Black, B.A., Sydeman, W.J., Bograd, S.J., Hazen, E.L., Santora, J.A., Wells, B.K., 2013. The north Pacific high and wintertime pre-conditioning of California Current productivity. Geophysical Research Letters 40, 541–546.
Shaw, C.T., Feinberg, L.R., Peterson, W.T., 2009. Interannual variations in the vital rates of copepods and euphausiids during the RISE study 2004–2006. Journal of Geophysical Research 114, C00B08.
Shaw, C.T., Peterson, W.T., Feinberg, L.R., 2010. Growth of *Euphausia pacifica* in the upwelling zone off the Oregon coast. Deep-Sea Research II 57, 584–593.
Shchepetkin, A.F., McWilliams, J.C., 2005. The regional ocean modeling system (ROMS): a split-explicit, free-surface, topography-following-coordinate oceanic model. Ocean Modelling 9, 347–404.
Smiles, M.C., Pearcy, W.G., 1971. Size structure and growth rate of *Euphausia pacifica* off the Oregon coast. Fishery Bulletin 69, 79–86.
Strathmann, R.R., 1967. Estimating the organic carbon content of phytoplankton from cell volume or plasma volume. Limnology and Oceanography 12, 411–418.
Strickland, J.D.H., 1965. Chemical Oceanography. Academic Press, London, England.
Sydeman, W.J., Bradley, R.W., Warzybok, P., Abraham, C.L., Jahncke, J., Hyrenbach, K.D., Kousky, V., Hipfner, J.M., Ohman, M.D., 2006. Planktivorous auklet *Ptychoramphus aleuticus* responses to ocean climate, 2005: unusual atmospheric blocking? Geophysical Research Letters 33, L22S09.
Thomas, A.C., Brickley, C., 2006. Satellite measurements of chlorophyll distribution during spring 2005 in the California Current. Geophysical Research Letters 33, L22S05.
Torres, J.J., Childress, J.J., 1983. Relationship of oxygen-consumption to swimming speed in *Euphausia pacifica*. 1. Effects of temperature and pressure. Marine Biology 74, 79–86.
Visser, A.W., 1997. Using random walk models to simulate the vertical distribution of particles in a turbulent water column. Marine Ecology Progress Series 158, 275–281.
Werner, F.E., Perry, R.I., Lough, R.G., Naimie, C.E., 1996. Trophodynamic and advective influences on Georges Bank larval cod and haddock. Deep-Sea Research II 43, 1793–1822.
Zar, J.H., 1999. Biostatistical Analysis. Prentice Hall, Upper Saddle River, New Jersey.